BioRisk

BioRisk 21: 1–10 (2023)
DOI: 10.3897/biorisk.21.101171

Research Article

Potential risk resulting from the influence of static magnetic field upon living organisms. Numerically simulated effects of the static magnetic field upon model complex lipids

Wojciech Ciesielski[1], Henryk Kołoczek[2], Zdzisław Oszczęda[2], Wiktor Oszczęda[2], Jacek A. Soroka[3], Piotr Tomasik[2]

1 *Institute of Chemistry, Jan Długosz University, 42 201 Częstochowa, Poland*
2 *Nantes Nanotechnological Systems, 59 700 Bolesławiec, Poland*
3 *Scientific Society of Szczecin, 71-481 Szczecin, Poland*
Corresponding author: Wojciech Ciesielski (w.ciesielski@interia.pl)

Abstract

Background: Recognising effects of static magnetic field (SMF) of varying flux density on flora and fauna is attempted. For this purpose, the influence of static magnetic field is studied for molecules of five complex lipids i.e. such as β-carotene, sphingosine, ceramide, cholesterol and phosphatidylcholine.

Methods: Computations of the effect of real SMF 0.0, 0.1, 1, 10 and 100 AMFU (Arbitrary Magnetic Field Unit; here 1AMFU > 1000 T) flux density were performed in silico (computer vacuum), involving advanced computational methods.

Results: SMF polarises molecules depending on applied flux density. Only β-carotene survives exposure to SMF of 10 and 100 AMFU without radical splitting of some valence bonds. Molecules of remaining lipids suffered radical cleavage of some bonds on exposure to SMF of 10 and 100 AMFU. Manipulation with applied flux density provides either inhibition or stimulation of biological functions of the lipids under study.

Conclusions: SMF destabilises complex lipids to the extent depending applied flux density. Biological functions of β-carotene are fairly sensitive to SMF, whereas only slight response to the effect of SMF is observed in case of sphingosine, ceramide and cholesterol. Enzymatic hydrolysis of phosphatidylcholine is stimulated by SMF regardless of the catalysed enzyme employed.

Key words: β-carotene, ceramide, cholesterol, phosphatidylcholine, sphingosine

Academic editor: Josef Settele
Received: 29 January 2023
Accepted: 20 July 2023
Published: 15 September 2023

Citation: Ciesielski W, Kołoczek H, Oszczęda Z, Oszczęda W, Soroka JA, Tomasik P (2023) Potential risk resulting from the influence of static magnetic field upon living organisms. Numerically simulated effects of the static magnetic field upon model complex lipids. BioRisk 21: 1–10. https://doi.org/10.3897/biorisk.21.101171

Introduction

Lipids play a diverse role in animal and plant organisms. They co-constitute biological membranes and triglycerides, located in adipose tissue, play a role in a major form of energy storage of animals and plants (Wang 2004; Dinasarapu et al. 2011; Berg at al. 2019).

Other functions involve transporting fat-soluble vitamins, oligosaccharides across cell membranes, participation in polysaccharide biosynthesis, activation of certain enzymes and formation of the basis for steroid hormones (Gohil and Greenberg 2009). Such role of lipids prompted us to extend this study. For that purpose, in our studies on the effect of Static Magnetic Field (SFM) upon biologically important components of plant and animal cells, we focused, amongst others, on lipids. In our former paper (Ciesielski et al. 2022), attention was paid to lipid acids and acyl glycerides. This paper is devoted to recognising the effect of SMF upon some model complex lipids, that is, β-carotene (carotenoids), cholesterol (sterols), sphingosine and ceramide (sphingolipids) and phosphatidylcholine (phospholipids) which are the most essential components of that group of compounds.

β-Carotene, a hydrocarbon with 11 conjugated double C=C bond systems is known as a lipid antioxidant (Anguelova and Warthesen 2008) and the precursor of A-vitamin. One molecule of β-carotene can be cleaved by the intestinal enzymes β,β-carotene-9',10'-mono-oxygenase into two molecules of vitamin A (Biesalski et al. 2007), whereas β,β-carotene 15,15'-mono-oxygenase does it eccentrically (Eroglu and Harrison 2013).

Sphingosine (2-amino-4-octadecene-1,3-diol) forms a primary part of cell membrane sphingolipids. Involving two type kinases, it is phosphorylated into sphingosine-1-phosphtate accounting for signalling lipids (Kataoka et al. 2005; Gergely et al. 2012; Huwiler and Zangemeister-Wittke 2017).

Ceramide (Fig. 3) is the sphingosine with a long fatty acids acylated amino group. It occupies cell membranes. Further modification with the phosphatidylcholine group leads to sphingomyelin constituting a lipid bilayer (Eder et al. 2022). Additionally, it participates in the differentiation, proliferation and programmed cell death mechanism (Siskind et al. 2002, 2006; Stiban et al. 2006). In this work as a simple model for calculation, except for long fatty acid amides, the formamide was accepted.

Cholesterol (Fig. 1) a specific unsaturated alcohol includes a cyclopentaphenanthrene (CPP) moiety. The C=C bond and the secondary hydroxyl group determine its chemical reactivity. Amongst others, cholesterol acts as a lipid antioxidant. The CPP moiety is common for steroids. Hence, apart from several physiological functions, it is a precursor of steroids – important biocatalysts formed enzymatically through steroidogenesis (Häggström and Richfield 2014).

Phosphatidylcholine, a phospholipid, is a major component of cell membranes and pulmonary surfactant. It is also a membrane-mediated cell signalling factor (Kanno et al. 2007). In this work, for simplification of calculations, a shorter 1,2-dibutyryl ester was taken.

The biological role of those molecules in living organisms of flora and fauna rationalises including them in our systematic studies on the influence of Static Magnetic Field (SMF) on biologically important elements of living cells. Thus, this report is devoted to advanced numerical simulations of SFM of 0, 0.1, 1, 10 and 100 AMFU (Arbitrary Field Density) arbitrary units performed for those molecules. The results could also be interesting for developing and functioning novel materials (Ramburrun et al. 2022) and systems (Smułek et al. 2023) of biomedical and food applications. Potentially, application of SMF of various field densities could offer either stimulation or inhibition of some processes as well as changing of the pathways.

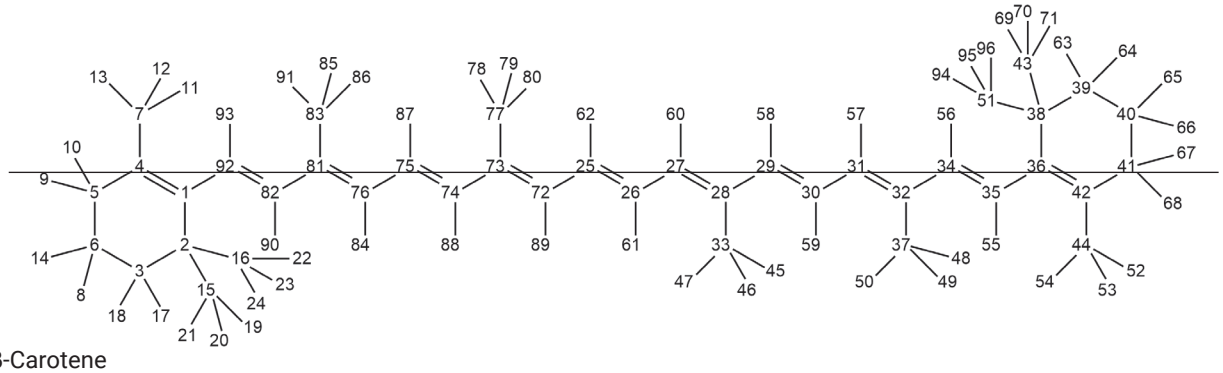

β-Carotene

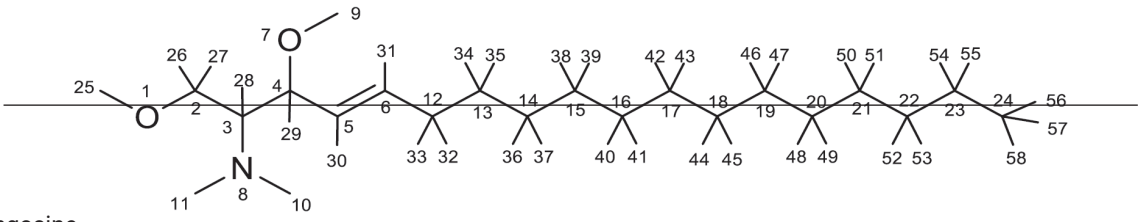

Sphingosine

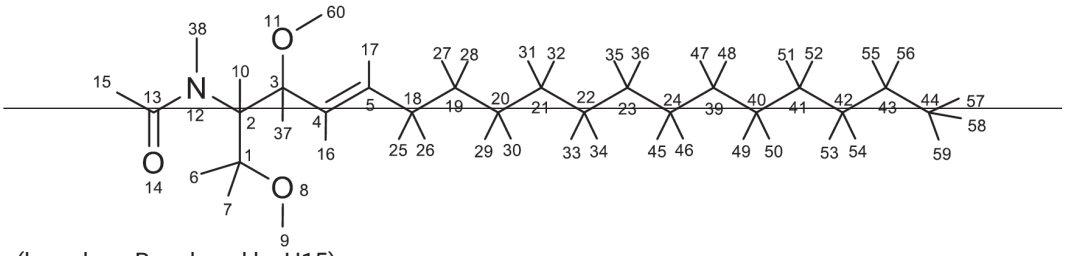

Ceramide (here: long R replaced by H15).

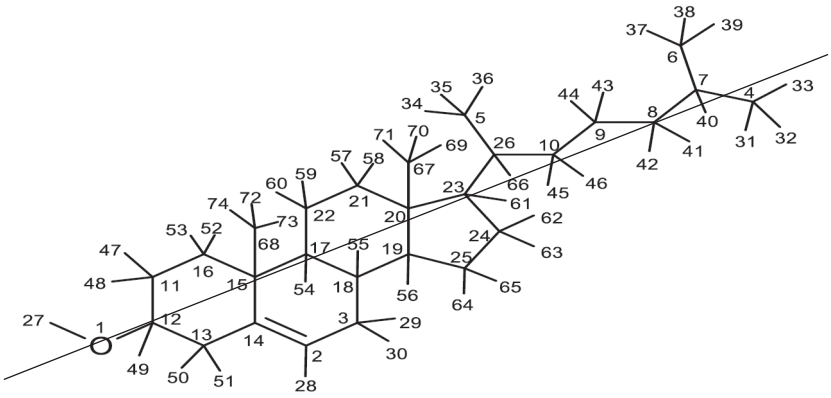

Cholesterol

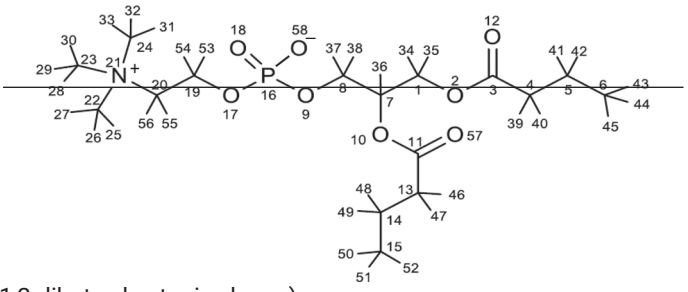

Phosphatidylcholine (here: 1,2-dibutyryl ester is shown).

Figure 1. Numbering atoms in the molecules of complex lipids. Orientation of molecules against x-axis is marked with red lines.

Materials and methods

Numerical computations

Computations of the effect of real SMF 0.0, 0.1, 1, 10 and 100 AMFU (Arbitrary Magnetic Field Units; here 1AFU > 1000 T) flux density were performed in silico (computer vacuum), involving advanced computational methods. The procedures follow those described in our former paper (Ciesielski et al. 2022).

Numbering atoms in particular molecules under consideration are presented in Fig. 1.].

Results and discussion

The effect of SMF of flux density from 0 to 100 AMFU upon heat of formation and dipole moment of five complex lipids is demonstrated in Table 1. Tables 2–8 present the effect of SMF in terms of charge density on selected atoms directly participating in biological activity of those lipids and bond lengths between those atoms. When the SMF of flux density generated the radical through extremely expanding some C-H bonds, only data for electron atoms carrying unpaired electrons are quoted. The data for the remaining atoms are omitted as they deal with molecules of radical character and, hence, with specific biological activity.

Table 1. Heat of formation (HF) [kJ.mole^{-1}] and dipole moment (DM) [D] of complex lipid molecules at flux density varying from 0 to 100 AMFU.

Molecule	HF [kJ.mole^{-1}] at flux density [AMFU]						DM [D] at flux density [AMFU]					
	0	0.1	1	10	100	$HF_0 - HF_{100}$	0	0.1	1	10	100	DM_{100}-DM_0
β-Carotene	-158	-151	-142	-106	-81	-77	0.25	0.31	0.71	0.93	1.53	1.28
Sphingosine	-1364	-1302	-1211	-1023	-817	-547	5.84	6.23	8.17	10.36	13.52	7.68
Ceramide	-1659	-1621	-1584	-1428	-985	-674	5.94	6.18	9.68	11.41	13.85	7.91
Cholesterol	-531	-501	-464	-403	-306	-225	1.62	1.78	2.06	3.57	6.51	5.89
Phosphatidylcholine	-1254	-1174	-1086	-964	-721	-533	2.48	2.94	3.85	5.13	12.15	9.67

Table 2. Charge density [a.u] on the C atoms of the conjugated double bond chain of β-carotene.

SMF [AMFU]	Charge density [a.u.] at SMF flux density [AMFU]																					
	C4	C1	C92	C82	C81	C76	C75	C74	C73	C72	C25	C26	C27	C28	C29	C30	C31	C32	C34	C35	C36	C42
0	-.065	-.282	.221	-.676	.351	-.416	-.202	-.245	.384	-.345	-.031	-.209	-.115	.198	-.171	-.310	-.205	.212	-.549	.199	-.262	-.095
0.1	-.115	-.249	.213	-.593	.321	-.388	-.225	-.221	.329	-.337	.002	-.191	-.108	.143	-.154	-.317	-.185	.170	-.568	.191	-.231	-.149
1	-.132	-.212	.209	-.763	.232	-.316	-.286	-.158	.166	-.338	.149	-.096	-.107	-.003	-.114	-.343	-.139	.083	-.725	.196	-.193	-.178
10	-.134	-.198	.207	-.781	.204	-.298	-.307	-.144	.126	-.416	.204	-.002	-.124	-.037	-.102	-.353	-.130	.061	-.743	.201	-.179	-.178
100	-.208	-.058	.200	-.488	.158	-.050	-.509	.005	-.371	-.161	-115	-.163	-.279	-.388	-.004	-.564	-.158	.001	-.396	.204	-.061	-.207

Table 3. Flux density dependent lengths [Å] of the double bonds potentially involved in oxidative reactions of β-carotene.

SMF [AMFU]	Bond length [Å] at flux density [AMFU]										
	C4=C1	C92=C82	C81=C76	C75=C74	C73=C72	C25=C26	C27=C28	C29=C30	C31=C32	C34=C35	C36=C42
0	.825	.825	.825	.825	.825	.825	.825.	.825	.825	.825	.825
0.1	.811	.841	.837	.840	.841	.784	.842	.842	.838	.842	.845
1	.888	.892	.878	.888	.889	.715	.899	.901	.887	.900	.899
10	.905	.911	.895	.909	.911	.674	.915	.923	.984	.920	.915
100	1.033	1.098	1.085	1.128	1.027	.782	1.023	1.117	1.076	1.091	1.026

Table 4. Flux density depende nt charge density [a.u.] on particular atoms in sphingosine.[a]

SMF [AMFU]	Charge density [a.u] on particular atoms at flux density [AMFU]																	
	H25	O1	C2	H26	H27	C3	H28	N8	H10	H11	C4	H29	O7	H9	=C5	H30	=C6	H
0	.205	-.350	-.006	.080	.072	-.018	.080	-.349	.140	.165	.069	.094	-.335	.208	-.209	.138	-.150	.120
0.1	.195	-.350	-.018	.085	.093	-.042	.092	-.339	.137	.151	.053	.107	-.340	.195	-.288	.134	-.162	.126
1	.305	-.326	-.001	.020	.062	-.062	.065	-.327	.123	.147	.020	.109	-.345	.224	-.181	.129	-.153	.109
10	*.204*	*-.090*																
100[b]	*.175*	*-.514*	*.140*	*.125*	*.119*	*.117*					*.114*	*.054*	*-.409*	*.208*				

[a]Values in italics relate to radical generated at given flux density.

[b]Also the following atoms carry free electrons: C18, H45, C19, H46, H47, C20, H48, H49, C21, H50, H51, C22, H52, H53, C23, H54, H55, C24, H56, H57, H58.

Table 5. Flux density dependent bond lengths [Å] between particular atoms in sphingosine.[a]

SMF [AMFU]	Bond lengths [Å] at flux density [AMFU]																
	H25-O1	O1-C2	C2-H26	C2-H27	C2-C3	C3-H28	C3-N8	N8-H10	N8-H11	C3-C4	C4-O7	O7-H9	C4-H29	C4-C5	C5-H30	C5-C6	C6-H31
0	0.950	1.430	1.090	1.090	1.510	1.090	1.470	1.010	1.010	1.540	1.430	0.960	1.090	1.520	1.080	1.340	1.080
0.1	0.952	1.502	1.095	1.092	1.573	1.092	1.520	1.084	1.085	1.567	1.514	0.952	1.093	1.517	1.074	1.365	1.084
1	1.993	1.278	1.513	1.467	1.591	1.208	1.558	1.028	1.035	1.016	1.640	1.430	1.297	1.421	1.208	1.388	1.164
10	*2.245*																
100	*2.509*		*2.727*	*2.506*		*2.040*							*2.180*				

[a]Values in italics relate to radical generated at given flux density.

Table 6. Effect of SMF flux density on the reaction site charge density of ceramide and selected bond atoms in that molecule.[a]

SMF [AMFU]	Charge density [a.u.] on the atoms of reacting hydroxyl group				
	O8	H9			
0	-.358	.212			
0.1	-.348	.199			
1	-.361	.320			
10	*-.392*	*.348*			
100	*-.398*	*.190*			
	Length of bonds [Å]				
	C8-H9	C1-H6	O11-H60	C44-H57	C44-H58
0	.950				
0.1	.962				
1	1.729				
10	*2.142*				
100	*2.508*	*2.161*	*2.037*	*2.351*	*2.301*

[a]Values in italics relate to radical generated at given flux density.

Discussion

A decrease in the negative value of heat of formation (Table 1) provides clear evidence for the destabilising effect of SMF upon the molecules of the lipids under consideration. That effect increased with an increase of the applied flux density. Accompanying increase in dipole moment of those molecules points to elongation of bonds and facility of polarisation of the molecules as the reason of destabilisation.

Table 7. Effect of SMF flux density on the reaction sites charge density of cholesterol and selected bond atoms in that molecule.[a]

SMF [AMFU]	Charge density [a.u.] on the reacting site atom										
	O1	H27	C2	H28	C14						
0	-0.333	0.251	-0.169	-0.131	-0.193						
0.1	-0.343	0.251	-0.170	-0.148	-0.194						
1	-0.389	0.382	-0.178	-0.142	-0.132						
	Bond length [Å]										
	C1-O27	C2-C14	C2-H28	O1-H27	C4-H33	C8-H39	C10-H46	C12-H49	C12-C13	C8-H41	C67-H69
0	1.430	1.336	1.000	0.960							
0.1	1.330	1.531	1.123	1.143							
1	1.199	1.385	1.142	1.518							
10	*2.162*				*2.496*	*2.138*	*2.059*				
100	*3.032*				*3.413*	*2.844*	*2.780*	*2.347*	*2.048*	*2.780*	*2.981*

[a]Values in italics relate to radical generated at given flux density.

Table 8. Effect of SMF flux density on the reaction sites charge density of phosphatidylcholine and selected bond atoms in that molecule.[a]

SMF [AMFU]	Charge density [a.u.] on the reacting site atom						
	O17	P16	O9	C3			
0	-0.556	1.731	-0.547	0.261			
0.1	-0.583	1.787	-0.578	0.271			
1	-0.636	1.891	-0.640	0.278			
	Bond length [Å]						
	P16-O17	P16-O9	C3-O2	P16-O18	C15-H51	C13-H47	C6-H45
0	1.790	1.790	1.360				
0.1	1.777	1.767	1.357				
1	1.795	1.717	1.360				
10	*1.932*	*1.777*	*1.369*	*2.064*	*2.597*		
100	*1.890*	*1.848*	*1.408*	*2.067*	*3.965*	*2.084*	*4.282*

[a]Values in italics relate to radical generated at given flux density.

The effect of SMF upon the stability of considered molecules increases in the order:

β-carotene < cholesterol < phosphatidylcholine < sphingosine < ceramide,

whereas the accompanying increase in the values of the dipole moment arranges in the order:

β-carotene < cholesterol <sphingosine < ceramide <phosphatidylcholine,

suggesting that the polarisation of the bonds is not the sole effect involved.

Amongst the five molecules under consideration (Fig. 1), β-carotene is the sole molecule surviving the effect of 100 AMFU flux density without generating radical split bonds. The remaining molecules already generated radicals on exposure to 10 AMFU (Tables 2–8).

The role of β-carotene as an antioxidant involves the whole conjugated double C=C bond system of the molecule. The process is due to trapping molecules of triplet oxygen following the radical mechanism. Such a process is stimu-

lated by a low polarisation of bonds accepting oxygen. The length of the double bonds in the β-carotene molecule increases with an increase of flux density (Table 3). It is accompanied by either an increase or decrease in the charge density on the atoms of the bonds depending on their positions in the chain.

This is surprising because it only applies to bonds located in the middle of the conjugated chain, in which, from a chemical point of view, all bonds are almost identical.

Review of Table 2 shows that, in such manner, some bonds turn more polar and some lose their original polarity in respect to that maintained in the molecule situated out of SMF. It suggests only a small effect of SMF upon a functioning β-carotene as an antioxidant and, depending on the applied flux density, varies the position of the reaction of that molecule with triplet oxygen. The enzymatically catalysed conversion of β-carotene into A vitamin involves a rupture of the C25=C26 double bond with the addition of the oxygen atom. Since that reaction follows an ionic mechanism, this reaction is stimulated by an increase in the polarity of that bond. At 0.1, 1 and 10 AMFU, the polarity of that bond increased in order to decrease dramatically at 100 AMFU. Another enzyme - β,β-carotene 15,15'-monooxygenase splits the C31=C32 bond, producing β-apo-10'-carotenal and β-ionone. SMF of 0.1, 10 and 100 AMFU decreased the polarity of that bond, whereas SMF of 1 AMFU increased its polarity (Table 2).

Biological function of sphingosine requires its introductory enzymatic phosphorylation at the O1 atom to convert the phosphorylated product into sphingomyelin (Fig. 2: (1)):

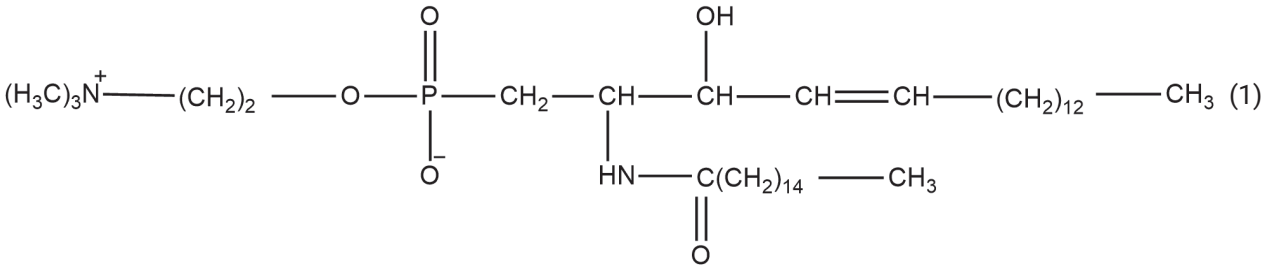

Figure 2. Structure of sphingomyelin.

The phosphorylation is stimulated by a high negative charge at the O1 atom. As shown in Table 4, SMF of 0.1 AMFU has no effect on that reaction and exposure to 1 AMHU slightly inhibits it. Exposure of sphingosine to 10 and 100 AMFU turns it to radicals. The positions of homolytic cleavage are marked in Tables 4 and 5.

The negative charge on the O8 atom in ceramide is slightly modulated by SMF. At 0.1 AMFU, it slightly decreases in order to slightly increase at 1 AMFU. Higher flux density produces radicals as shown in Table 6.

SMF of 0.1 AMFU subtly decreases the polarity of the C2=C14 bond stimulating in this manner the role of cholesterol as antioxidant, but at 1 AMFU, the polarity of that bond increases, inhibiting that role of cholesterol. Simultaneously, the negative charge density on the O8 atom increases, stimulating reactivity of the OH group. SMF of 10 and 100 AMFU generates radical cleavage of certain bonds (Table 7).

There are three reaction sites in phosphatidylcholine, each employed by another enzyme (Fig. 3)

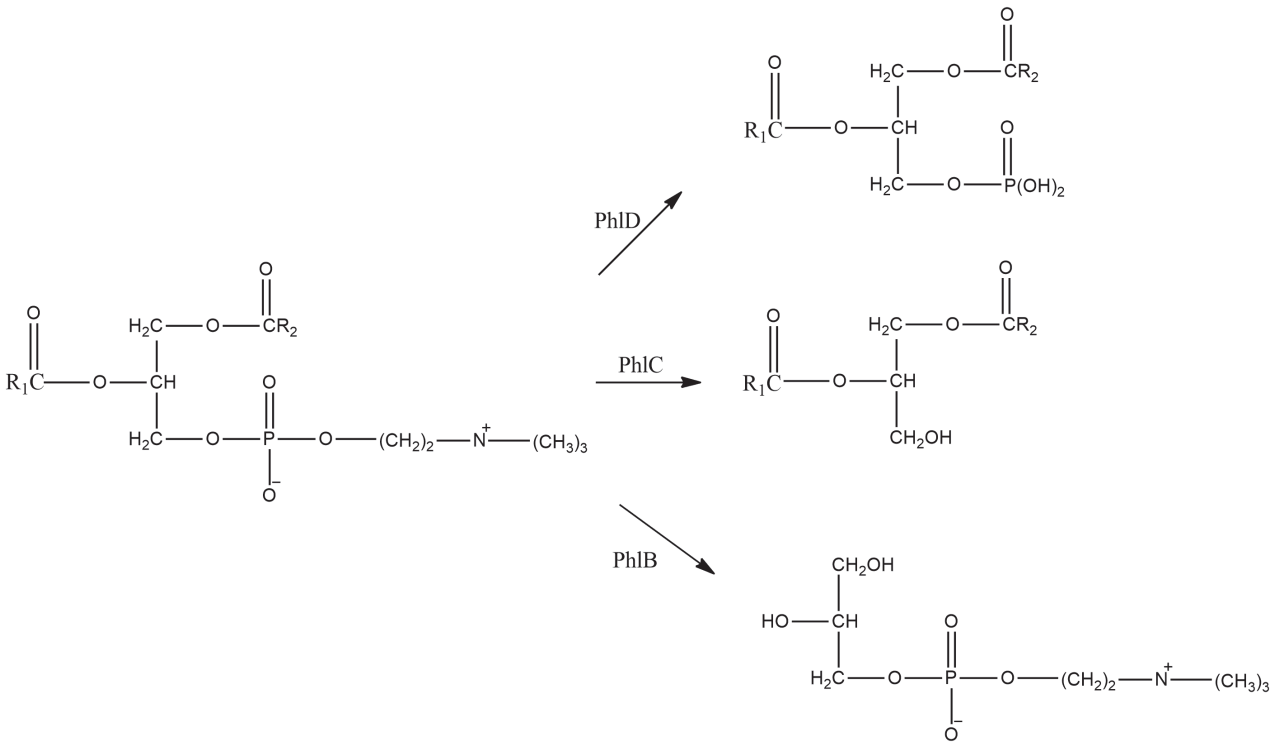

Figure 3. Hydrolysis of phosphatidylcholine with B, C and D phospholipases (Phl).

B, D and C phospholipases belong to the group of hydrolases. Their action should be stimulated by a high positive charge density on the P16 atom, whereas the hydrolysis with B phospholipase should be stimulated by a high positive charge density on the C3 atom. Data in Table 8 identify that SMF of 0.1 and 1 stimulated all three enzymatic hydrolyses. SMF of 10 and 100 AMFU generates radicals by splitting bonds shown in that Table.

Conclusions

In terms of heat of formation, SMF destabilises molecules of the lipids under study. An increase in the polarity of the molecules is the main reason of observed effect. Amongst five complex lipids under consideration, only β-carotene survives exposure to 10 and 100 AMFU without radical cleavage of some bonds. SMF has a diverse effect upon a functioning β-carotene as antioxidant. Depending on the applied flux density, there is a variation in the position of the reaction of that molecule with triplet oxygen. The enzymatically catalysed conversion of β-carotene into A vitamin is stimulated by an increase in the polarity of that bond. At 0.1, 1 and 10 AMFU, the polarity of that bond increased in order to decrease dramatically at 100 AMFU. The reaction catalysed by β,β-carotene 15,15'-monooxygenase leading to β-apo-10'-carotenal and β-ionone is inhibited by SMF of 0.1, 10 and 100 AMFU and stimulated by SMF of 1 AMFU.

The phosphorylation of sphingosine, which is responsible for biological function of that lipid, remains unaffected by SMF of 0.1 AMFU and slightly inhibited by SMF of 1 AMFU. The biological function of ceramide is only slightly modulated by SMF. Flux density of 0.1 AMFU slightly inhibits it, whereas a weak stimulation takes place at 1 AMFU.

SMF of 0.1 AMFU subtly stimulates the role of cholesterol as antioxidant, but at 1 AMFU, inhibition of that role is observed. Simultaneously, the reactivity of the primary hydroxyl group is stimulated at SMF of 0.1 and 1 AMFU. SMF of 0.1 and 1 AMFU stimulates hydrolysis of phosphatidylcholine with B, C and D phospholipases.

The presented results concern only changes caused by SMF in selected substrates, but all bioprocesses also involve enzymes. They are also exposed to SMF. We shall address that problem in our subsequent works.

Additional information

Conflict of interest

The authors have declared that no competing interests exist.

Ethical statement

No ethical statement was reported.

Funding

No funding was reported.

Author contributions

Conceptualization: WC, PT. Formal analysis: JAS, HK, WC. Investigation: WC, ZO. Methodology: WC. Writing - original draft: WC. Writing - review and editing: PT.

Data availability

All of the data that support the findings of this study are available in the main text.

References

Anguelova T, Warthesen J (2008) Degradation of lycopene, α-carotene, and β-carotene during lipid peroxidation. Journal of Food Science 65(1): 71–75. https://doi.org/10.1111/j.1365-2621.2000.tb15958.x

Berg JM, Tymoczko JL, Gatt Jr GJ, Stryer L (2019) Biochemistry (9th ed). W.H Freeman and Company, New York.

Biesalski HK, Chichili GR, Frank J, von Lintig J, Nohr D (2007) Conversion of beta-carotene to retinal pigment. Vitamins and Hormones 75: 117–130. https://doi.org/10.1016/S0083-6729(06)75005-1

Ciesielski W, Kołoczek H, Oszczęda Z, Soroka JA, Tomasik P (2022) Potential risk resulting from the influence of static magnetic field upon living organisms. Numerically simulated effects of the static magnetic field upon fatty acids and their glycerides. BioRisk. [In press]

Dinasarapu AR, Saunders B, Ozerlat I, Azam K, Subramaniam S (2011) Signaling gateway molecule pages—A data model perspective. Bioinformatics (Oxford, England) 27(12): 1736–1738. https://doi.org/10.1093/bioinformatics/btr190

Eder S, Hollmann C, Mandasari P, Wittmann P, Schumacher F, Kleuser B, Fink J, Seibel J, Schneider-Schaulies J, Stigloher C, Beyersdorf N, Dembski S (2022) Synthesis and characterization of ceramide-containing liposomes as membrane models for different T cell subpopulations. Journal of Functional Biomaterials 13(3): 111. https://doi.org/10.3390/jfb13030111

Eroglu A, Harrison EH (2013) Carotenoid metabolism in mammals, including man: Formation, occurrence, and function of apocarotenoids. Journal of Lipid Research 54(7): 1719–1730. https://doi.org/10.1194/jlr.R039537

Gergely P, Nuesslein-Hildesheim B, Guerini D, Brinkmann V, Traebert M, Bruns C, Pan S, Gray NS, Hinterding K, Cooke NG, Groenewegen A, Vitaliti A, Sing T, Luttringer O, Yang J, Gardin A, Wang N, Crumb Jr WJ, Saltzman M, Rosenberg M, Wallström E (2012) The selective sphingosine 1-phosphate receptor modulator BAF312 redirects lymphocyte distribution and has species-specific effects on heart rate. British Journal of Pharmacology 167(5): 1035–1047. https://doi.org/10.1111/j.1476-5381.2012.02061.x

Gohil VM, Greenberg ML (2009) Mitochondrial membrane biogenesis: Phospholipids and proteins go hand in hand. The Journal of Cell Biology 184(4): 469–472. https://doi.org/10.1083/jcb.200901127

Häggström M, Richfield D (2014) Elevated estrogens are a risk factor for #male breast cancer-finally a study looks at this important issue Wikiversity. Journal of Medicine 1(1). https://doi.org/10.15347/wjm/2014.005

Huwiler A, Zangemeister-Wittke U (2017) The sphingosine 1-phosphate receptor modulator fingolimod as a therapeutic agent: and new perspectives. https://doi.org/10.1016/j.pharmthera.2017.11.001

Kanno K, Wu MK, Agate DA, Fanelli BK, Wagle N, Scapa EF, Ukomadu C, Cohen DE (2007) Interacting proteins dictate function of the minimal START domain phosphatydylcholine transfer protein/StarD2. The Journal of Biological Chemistry 282(42): 30728–30736. https://doi.org/10.1074/jbc.M703745200

Kataoka H, Sugahara K, Shimano K, Teshima K, Koyama MA, Fukunari AK, Chiba K (2005) FTY720, Sphingosine 1-phosphate receptor modulator, ameliorates experimental autoimmune encephalomyelitis by inhibition of T cell infiltration. Cellular & Molecular Immunology 2(6): 437–448. https://pubmed.ncbi.nlm.nih.gov/16426494/

Ramburrun P, Riaz A, Khan RA, Yahya E, Choonara YE (2022) Design, preparation, and functionalization of nanobiomaterials for enhanced efficacy in current and future biomedical applications. Nanotechnology Reviews 11(1): 1802–1826. https://doi.org/10.1515/ntrev-2022-0106

Siskind LJ, Kolesnick RN, Colombini M (2002) Ceramide channels increase the permeability of the mitochondrial outer membrane to small proteins. The Journal of Biological Chemistry 277(30): 26796–26803. https://doi.org/10.1074/jbc.M200754200

Siskind LJ, Kolesnick RN, Colombini M (2006) Ceramide forms channels in mitochondrial outer membranes at physiologically relevant concentrations. Mitochondrion 6(3): 118–125. https://doi.org/10.1016/j.mito.2006.03.002

Smułek W, Grząbka-Zasadzińska A, Kilian A, Ciesielczyk F, Borysiak S, Baranowska HM, Walkowiak K, Kaczorek E, Jarzębski M (2023) Design of vitamin-loaded emulsions in agar hydrogel matrix dispersed with plant surfactants. Food Bioscience 53: 102559. https://doi.org/10.1016/j.fbio.2023.102559

Stiban J, Fistere D, Colombini M (2006) Dihydroceramide hinders ceramide channel formation. Implications on apoptosis. Apoptosis 11(5): 773–780. https://doi.org/10.1007/s10495-006-5882-8

Wang X (2004) Lipid signalling. Current Opinion in Plant Biology 7(3): 329–336. https://doi.org/10.1016/j.pbi.2004.03.012

BioRisk

BioRisk 21: 11–18 (2023)
DOI: 10.3897/biorisk.21.108551

Short Communication

Biomonitoring with bryophytes in managed forested areas. Three examples from the southern Italian Apennines

Carmine Colacino[1]

1 *Scuola di Scienze Agrarie, Forestali, Alimentari e Ambientali (SAFE), Università degli Studi della Basilicata, Potenza, Italy*
Corresponding author: Carmine Colacino (carmine.colacino@unibas.it)

Abstract

Three sites in the southern Italian Apennines were selected to assess correlation between forest structure and bryophyte flora. In two of the sites, the Index of Air Purity (IAP)–based on cover data of epiphytic bryophytes–was evaluated. The results show that bryophyte populations–and consequently IAP–are affected by forest structure and development, and that studies including different sites require a precise assessment of silvicultural characteristics to allow comparisons. Indicator values of mosses and liverworts were also taken into consideration in characterizing ecologically the three sites.

Key words: Bryophyte Flora, forest structure, IAP, indicator values, silviculture

Introduction

Bryophytes are a popular tool for the assessment of air quality in polluted urban areas, showing, together with lichens, all the necessary characteristics for a good bioindicator. They are sensible to polluting agents, stay in place in the area of study, have wide distribution and a life cycle sufficiently long, and they can accumulate pollutants in their body (Aleffi 1998; Govindapyari et al. 2010). De Sloover proposed in 1964 an Index of Atmospheric Purity (IAP) to assess air pollution and based on cover data of epiphytic lichens (De Sloover 1964; De Sloover and LeBlanc 1968) and epiphytic bryophytes (LeBlanc and De Sloover 1970). The IAP is extensively applied in cities and urban areas (*e.g.*, Aleffi 1992; Dymytrova 2009; Zechmeister and Hohenwallner 2006) to supplement static and mobile monitors (for CO, CO_2, SO_2, O_3, NO_x), or satellite monitoring systems to assess particulate matter pollution, ground-level ozone, carbon monoxide and other major contaminants in wider areas. The limit of these monitoring devices is that they do not give information about the effects of air contaminants at the ecological level. The aim of this study is to verify the use of the IAP method (selected because of its widespread use and the possibility to have comparable results) in the assessment of environmental pollution in managed forested environments. Cryptogamic communities are conditioned by the developmental stage of the forest (Barkman 1958), and bryophytes, in particular, are important ecological components of managed forests. Bryophyte flora and vegetation provide information on the conditions of a forested area, its structure, ecology and climate at a given time

OPEN ACCESS

Academic editor: Pavel Stoev
Received: 23 June 2023
Accepted: 28 September 2023
Published: 27 October 2023

Citation: Colacino C (2023) Biomonitoring with bryophytes in managed forested areas. Three examples from the southern Italian Apennines. BioRisk 21: 11–18. https://doi.org/10.3897/biorisk.21.108551

(Brunialti et al. 2010). To further characterize ecologically the areas under study, and to evaluate the effectiveness of the Indicator Values of Mosses and Liverworts (Düll 1991), non-epiphytic bryophyte species have been considered. These indicator values were originally developed for Central Europe, but they appear to be usable also in internal mountain areas of southern Italy. The numerical values of these ecological indicators (varying from 1 to 9) are: Light number (L), from deep shade plants to full light plants. Temperature number (T), from cold to extreme warm indicators (from alpine to lowland, or from the Arctic to the Mediterranean zone). Continentality number (C), from euoceanic to eucontinental (from the Atlantic coast to the interior of Eurasia). Moisture number (M), from great dryness to permanently wet or sprayed, near waters or waterfalls, in water). Reaction number (R), from strong acid to base and lime indicators. The Median value is then calculated. Chorological values were also considered, but are not presented here.

Material and methods

The study sites were analyzed by determining their flora (bryological and vascular), climate, geology, pedology. Plots were established and silvicultural parameters calculated (tree-structure and developmental stage).

The IAP (sites A and B) was calculated according to the method presented by LeBlanc and De Sloover (1970) as partially modified by Nimis (1990). In particular, (1) a 60 x 50 cm grid–divided into 20 units of 10 x 15 cm–was placed on the trunk of each tree at a height (lower side) of 80–100 cm, in areas with the highest bryophyte density; (2) The IAP was calculated based on the following formula:

$$IAP = \sum_{i=1}^{n} (Qi \times fi / 10),$$

where f_i is an index of frequency/cover varying from 1 to 5; Q_i is the number of species accompanying any other species in each relevée (a factor of resistance to pollution).

The division by 10 is arbitrary and was indicated in the original formula by LeBlanc and De Sloover (1970) to obtain smaller numbers. These values are based on the diversity of epiphytic bryophyte populations, on the resistance to pollution of each species, on the phorophytes, and, in our case, on the forest structure and stage of development. Values of IAP recorded in the literature in urban areas vary according to the distance from the pollution source and the ecological conditions of the site (Nimis 1999). Values may vary from close to zero (indicating air pollution) up to values of 50 or more (indicating lack of air pollution).

The bryophyte vegetation was considered in three sites: (Site A) a managed forested area with *Quercus cerris* L. (Turkey oak) prevalent, and *Quercus pubescens* Willd. (Downey oak) sporadic, near an Oil hub; (Site B) a forested area with *Fagus sylvatica* L. (Beech). The IAP was determined in both sites; (Site C) a mountain area with a *Fagus sylvatica-Abies alba* Mill. (Beech-Silver fir) coenosis. The Indicator Values of mosses and liverworts were calculated for all three sites.

Site A

The area of study is situated in a plain near the Oil Hub of Viggiano (Locality Refesa, Province of Potenza, Basilicata) in the Valley of the river Agri at an altitude of

610–620 m, in the heart of the southern Apennines. The geology is complex, in the area considered there is limestone, shale, flysch, and varicolored clay. The soil is various–of alluvial origin under the plots. Climate is Mediterranean with dry summers and the rains occurring mainly from October to February (max. in November, 87.3 mm). Average annual temperature is 12.4 °C. Coldest month average 4.5 °C. Warmer month average 21.6 °C. The De Martonne Aridity Index was calculated, its value (24.3) indicating a sub-humid climate. Overall, a Mediterranean climate of the sub-humid type. According to a recent vegetation classification of Italy this area is included in the temperate region, meso-temperate zone, southern Apennines, neutro-subacidophilous series of Turkey oak (Di Pietro et al. 2010).

Three plots were selected and the usual dendrometry parameters measured (height, dbh, growth estimate, basal area, etc.). The wood is relatively young and the prevalent species is Turkey oak, with the sporadic presence of Downey oak. Sampling occurred in 2003 and then again in 2008. In the first plot the management is simple coppice (low forest) with an average age of 13–14 years (in 2003, 18–19 in 2008). The second plot is inwards with older trees (about 30 years, then 35) and represent an aged coppice in conversion into high forest. The third plot is a coppice-with standards stand, with larger diameters and more spaced trees.

Site B

Mount Paratiello is situated to the west of the town of Muro Lucano (Province of Potenza, Basilicata), in the southern Apennines, in the basin of torrents–some with a more or less continuous flow of water, others with seasonal regimes–tributary to the river Sele. The altitudes vary from 500 to 1400 m. Prevalent expositions N, NE, NW. Geologically young, the erosion has exposed limestone from the Cretaceous. Soils belong to the southern brown earths. The climate is Mediterranean with dry summers and rains occurring mainly from September to March (max. in December, 163 mm). Average annual temperature is 14.3 °C. Coldest month average 2.2 °C. Warmer month average 30.4 °C (data 2000–2010). The Aridity Index of De Martonne is 46.8 indicating a humid climate. According to a recent vegetation classification of Italy this area is included in the temperate region, lower supra-temperate zone, southern Apennines, neutro-basiphilous series of beech (Di Pietro et al. 2010).

The main species in the plots is *Fagus sylvatica* (beech). The forest is quite old and was exploited heavily in the past (1700–1860). Some studies (e.g., Susmel 1957) concluded it should be managed to get an uneven-aged structure, but it has always been managed as an even-aged system. Two plots were selected, at 1356 m, and at 1423 m. The main difference between the two plots is the time of last cutting, more recent in the first one (trees with smaller diameters). Another factor affecting the plots is the slope, steeper at 1424 m–at the tree vegetational limit, and more subject to erosion.

Site C

The population of silver fir on the northern slopes of Mount Motola (Teggiano, Province of Salerno, Campania) represents the most important relict association of silver fir in Campania, where it is associated with the beech. It is included in

the National Park of Cilento and Vallo di Diano, one of the largest in Italy. The habitat belongs to the group of Mediterranean deciduous forests: "Apennine beech forests with *Abies alba*". At lower altitudes (800 to 900 m) *Corylus avellana* L. (Hazelnut) is found in areas previously cultivated. The slopes show a series of terraces supported by stone-walls, eroded by flowing rainwaters. At around 1000 m sparse and isolated individuals of silver fir are found, mostly in hollows and in areas of difficult access. The hazelnut stands still maintain the original density of plantation and the stools feature a high number of shoots, which form a dense and continuous cover not colonized by other species. This area (in the submontane belt up to about an altitude of 800–900 m) belongs to the mixed forest of mesophile and meso-xerophile broadleaf trees (e.g., Pignatti et al. 2004) made up by maples (*Acer campestre* L., *Acer opalus* Mill. subsp. *obtusatum* (Waldst. & Kit. ex Willd.) Gams, *Acer lobelii* Ten.), European hop hornbeam (*Ostrya carpinifolia* Scop.), Chestnut (*Castanea sativa* Miller), Italian alder (*Alnus cordata* (Loisel.) Desf.), Bigleaf linden (*Tilia platyphyllos* Scop.). Climate is cold-humid, Temperate Oceanic, without noticeable temperature extremes. Rains are well distributed during the year. Soils are well aerated brown earths, with an abundant litter layer and good water retention. Geologically limestone prevails (Saracino et al. 2005; Cipollaro and Colacino 2005). According to a recent vegetation classification of Italy this area is included in the temperate region, lower supra-temperate zone, southern Apennines, neutro-basiphilous series of beech (Filesi et al. 2010).

Results

The main silvicultural and bryological (Indicator Values) results are presented for each of the areas considered. (Plots have a diameter of 20 m, and are located at a distance of 60 m one from the other.)

P=Plot; TBA=Total Basal Area (m^2); ABA=Average Basal Area (m^2); AD Average Diameter (cm, min.-max). IAP=Index of Air Purity (Sites A and B only).

Site A – *Quercus cerris* (Turkey oak)

Year 2003:

- P1: #trees 402 – TBA 1.873 – ABA 0.005 – AD 8 (03–21) – IAP=0.32
- P2: #trees 278 – TBA 2.581 – ABA 0.009 – AD 11 (03–36) – IAP=0.43
- P3: #trees 143 – TBA 2.568 – ABA 0.018 – AD 15 (06–31) – IAP=0.37

Year 2008:

- P1: #trees 422 – TBA 3.597 – ABA 0.008 – AD 10.5 (05–19.0) – IAP=1.10
- P2: #trees 243 – TBA 4.120 – ABA 0.023 – AD 14.5 (05–37.0) – IAP=0.80
- P3: #trees 167 – TBA 3.909 – ABA 0.018 – AD 17.0 (05–37.0) – IAP=0.70
- P4: #trees 364 – TBA 1.962 – ABA 0.005 – AD 8.0 (05–23.5) – IPA= NC

Indicator Values of mosses and liverworts:

- L = 7 (Semi-light plants, in full indirect light, but also occurring in shade). T = 4 (between moderate warm and cool). C = 5 (Intermediate, between

sub-Mediterranean and sub-boreal). M = 4 (places moderately fresh becoming dry for long periods). R = 6 (between moderate acid and weakly acid to weakly basic indicator).

Site B – *Fagus sylvatica* (Beech)

- P1 1356 m: #trees 288 – TBA 4.635 – ABA 0.016 – AD 14.5 (5–69) – IAP=2.2
- P2 1423 m: #trees 152 – TBA 6.601 – ABA 0.043 – AD 23.0 (5–60) – IAP=4.0

Indicator Values of mosses and liverworts:

- L = 7 (Semi-light plants, in full indirect light, but also occurring in shade). T = 3 (cool). C = 5 (Intermediate, between sub-Mediterranean and sub-boreal). M = 4 (places moderately fresh becoming dry for long periods). R = 6 (between moderate acid and weakly acid to weakly basic indicator).

Site C – *Fagus sylvatica-Abies alba* (Beech-Silver fir) coenosis

- P1 900 m: #trees 438 – TBA 18,4 – ABA 0.042 – AD 23.1 (Beech)
- P1 900 m: #trees 275 – TBA 18,5 – ABA 0.067 – AD 29.3 (Silver fir)
  - Sporadic presence of Bigleaf linden, Hungarian maple and Chestnut: TBA 3.75.
- P2 1100 m: #trees 703 – TBA 30.2 – ABA 0.043 – AD 23.4 5 (Beech)
  - Sporadic presence of European hop hornbeam, Hungarian maple and Italian alder. Silver fir (sub-canopy) TBA 2.5.

Indicator Values of mosses and liverworts:

- 700–900 m: L = 5 (semi shade plants), T = 5 (moderate warmth), C=5 (intermediate), M = 7 (moisture), R =7 (weakly acid to weakly basic).
- 1000–1300 m: L = 5 (as above), T = 4 (sub-Oceanic), C = 5 (as above), M = 7 (as above), R = 6 (between moderate acid and weakly acid to weakly basic).

In this site the study has been focused on the bryophyte flora and the silvicultural aspects, from lower to higher altitudes. No IAP was calculated.

Discussion

Site A – The silvicultural data show there has been, as expected, an increase in the average diameters in the three plots after 5 years, which is reflected also in the values of total and average basal areas. This increase in diameter has affected the number of epiphytic bryophyte species recorded. Downey oak was not considered in the measurements, being a much better phorophyte. Plot 4 of 2008 was made up of very young plants with smaller diameters, too small to have any significant epiphytic vegetation. IAP could not be calculated (NC). Overall, TBA values appear low, indicating a forest in the first stages of development. The Indicator values of mosses and liverworts–re-

flecting the general ecological conditions of the site–have not changed from 2003 to 2008, as expected.

Site B – Plot 1 was cut more recently than Plot 2, as indicated, altering the number of epiphytes capable to attach and grow on the bark, and resulting in different IAP values. These values, in both plots, are quite low, not much different from those obtained in Site A which was exposed to pollution. This may be due to the type of forest management applied, with younger trees prevailing, and lacking the time to reach an equilibrium (as shown by low TBA values). The Indicator values appear to be almost identical in the two plots. Plot 1 has the same values, while Plot 2 diverges only for M = 3 (dryness); this is due to its position near the tree line and the uppermost montane grassland (edge effect) exposing to the sun the bryophytes from the inside, as it was shown by Hylander (2005).

Site C – This forest is characterized by silver firs. Beeches become more frequent in the higher parts of the submontane belt, as compared to other broadleaf trees (Plot 1). In this belt, the presence of all diametrical classes of silver firs in reproductive age has been recorded (an abundant production of cones was observed during Fall 2002). Silver firs here are taller than beeches, and their canopy is directly exposed to sun rays. Their spatial distribution varies from isolated plants within a stand of beeches, to pure populations with an extension of even a few thousand square meters exhibiting the micro-environmental conditions of pure silver fir forests. At higher altitudes (Plot 2) beeches become the dominant trees and silver firs almost disappear (even though old big stumps and rotting logs are still visible). Silver firs are still relatively abundant in the sub-canopy layers as individuals of about 1–4 m of height in a "waiting" phase, many with the vegetative apex damaged by grazing or by contact with branches of higher trees. The Indicator values show that bryophytes of xeric or Mediterranean environments prevail at lower elevations, while at higher elevations, at the tree line, species with a sub-Oceanic (and sub-Mediterranean) ecology prevail, as expected given the different ecological conditions previously indicated.

Conclusions

The values of IAP obtained in this study need consideration, and an explanation. These values are lower in Site A, near a source of pollution, and higher in site B, with no apparent pollution source, as expected. The IAP values in site B, however, are much lower than those normally obtained in unpolluted urban areas. This may be related to the silvicultural management systems applied, with frequent cutting of trees and resulting low TBAs, altering adversely bryophyte diversity because of their vulnerability to microclimatic changes (Perhans et al. 2009). Further study is required to compare IAP values from forest sites to those obtained in urban areas; the determination of correction factors (possibly based on TBA values, and phorophyte selection) is necessary. A preliminary strategy–limited to forested areas, would be to consider stands at the same stage of development and with comparable management systems, better if aged (Hébrard 1989). The effectiveness of the Indicator values for mosses and liverworts for the areas considered was verified both spatially (sites A, B, and C) and temporally (site A).

Acknowledgments

I thank colleagues and students who assisted me in the field in some of the studies reported here. Among them, I thank in particular, Enza Evangelista, Carmine D'Avella, and Filippo Verova.

Additional information

Conflict of interest

The authors have declared that no competing interests exist.

Ethical statement

No ethical statement was reported.

Funding

Financial support from my Department (SAFE) is kindly acknowledged.

Author contributions

The author solely contributed to this work.

Author ORCIDs

Carmine Colacino https://orcid.org/0000-0002-2675-8835

Data availability

All of the data that support the findings of this study are available in the main text or Supplementary Information.

References

Aleffi M (1992) Flora briologica e qualità dell'aria nella città di Jesi (Marche – Italia centrale). Archivio Botanico Italiano 67: 128–140.

Aleffi M (1998) Bioindicatori a livello di organismi vegetali: le Briofite. In: Sartori F (Ed.) Bioindicatori ambientali, 102–112.

Barkman JJ (1958) Phytosociology and Ecology of Cryptogamic Epiphytes. Van Gorcum, Assen, 628 pp.

Brunialti G, Frati L, Aleffi M, Marignani M, Rosati L, Burrascano S, Ravera S (2010) Lichens and bryophytes as indicators of old-growth features in Mediterranean forests. Plant Biosystems 144(1): 221–233. https://doi.org/10.1080/11263500903560959

Cipollaro S, Colacino C (2005) Bryoflora of the beech-silver fir coenosis of Mount Motola (National Park of Cilento & Vallo di Diano) – Teggiano (Salerno, S-Italy). Flora Mediterranea 15: 385–396.

De Sloover J (1964) Végétaux épiphytes et pollution de l'air. Rev. Questions scientifiques 25: 531–561.

De Sloover J, LeBlanc F (1968) Mapping of atmospheric pollution on the basis of lichen sensitivity. In: Misra R, Gopal B (Eds) Proceedings of the Symposium in Recent Advances in Tropical Ecology. Banaras Hindu Univ., Varanasi, 42–56.

Di Pietro R, Fascetti S, Filibeck G, Blasi C (2010) Le serie di vegetazione della regione Basilicata. In: Blasi C (Ed.) La Vegetazione d'Italia. Palombi, Roma, 375–389.

Düll R (1991) Indicator Values of Mosses and Liverworts. In: Ellenberg H, Weber E, Düll R, Werner W, Pauliben D (Eds) Indicator Values of Plants in Central Europe. Goltze, Gottingen, 175–214.

Dymytrova L (2009) Epiphytic lichens and bryophytes as indicators of air pollution in Kyiv city (Ukraine). Folia Cryptogamica Estonica 46: 33–44.

Filesi L, Rosati L, Paura B, Cutini M, Strumia S, Blasi C (2010) Le serie di vegetazione della regione Campania. In: Blasi C (Ed.) La Vegetazione d'Italia. Palombi, Roma, 351–373.

Govindapyari H, Leleeka M, Nivedita M, Uniyal PL (2010) Bryophytes: Indicators and monitoring agents of pollution. NeBio 1: 35–41.

Hébrard JP (1989) Étude comparée de la végétation bryophytique des troncs de chêne vert et de chêne pubescent (Peuplement âgés) dans la forêt domaniale de La Gardiole de Rians (Var, France). Cryptogamie. Bryologie, Lichenologie 10: 253–266.

Hylander K (2005) Aspect modifies the magnitude of edge effects on bryophyte growth in boreal forest. Journal of Applied Ecology 42(3): 518–525. https://doi.org/10.1111/j.1365-2664.2005.01033.x

LeBlanc F, De Sloover J (1970) Relation between industrialization and the distribution and growth of epiphytic lichens and mosses in Montreal. Canadian Journal of Botany 48(8): 1485–1496. https://doi.org/10.1139/b70-224

Nimis PL (1990) Air quality indicators and indices: the use of plants as bioindicators for monitoring air pollution. In: Colombo AG, Premazzi G (Eds) Proc. Workshop Indicators and Indices for Environmental Impact Assessment and Risk Analysis. Ispra (Italy), May 1990, JRC (Ispra), 93–126.

Nimis PL (1999) Linee-guida per la bioindicazione degli effetti dell'inquinamento tramite la biodiversità dei licheni epifiti. In: Piccini C, Salvati S (Eds) Atti Workshop Biomonitoraggio Qualità dell'Aria sul Territorio Nazionale. ANPA Atti 2: 267–277.

Perhans K, Appelgren F, Jonsson F, Nordin U, Söderström B, Gustafsson L (2009) Retention patches as potential refugia for bryophytes and lichens in managed forest landscapes. Biological Conservation 142(5): 1125–1133. https://doi.org/10.1016/j.biocon.2008.12.033

Pignatti G, Terzuolo PG, Varese P, Semerari P, Lombardi VN (2004) Criteri per la definizione di tipi forestali nei boschi dell'Appennino meridionale. Forest@ 1: 112–127. https://doi.org/10.3832/efor0229-0010112

Saracino A, Colacino C, Esposito L, Curcio B, Cipollaro S (2005) Il consorzio faggio-abete bianco del Monte Motola di Teggiano (SA): Aspetti selvicolturali e primo contributo alla brioflora. S.I.S.E.F. Atti 4: 165–171.

Susmel L (1957) Premesse storico-climatiche e bio-ecologiche alla selvicoltura della foresta montana appenninica. Annali Accademia economico-agraria dei Georgofili 4: 3–42.

Zechmeister HG, Hohenwallner D (2006) A comparison of biomonitoring methods for the estimation of atmospheric pollutants in an industrial town in Austria. Environmental Monitoring and Assessment 117(1–3): 245–259. hhttps://doi.org/10.1007/s10661-006-0991-y

BioRisk

BioRisk 21: 19–28 (2023)
DOI: 10.3897/biorisk.21.111983

Research Article

Prospects and possibilities of using Raman spectroscopy for the identification of *Pseudomonas aeruginosa* from turtle *Emys orbicularis* (Linnaeus, 1758) skin

Aleksandrs Petjukevičs[1], Inta Umbraško[1], Natalja Škute[1]

1 *Institute of Life Sciences and Technology, Daugavpils University, Parades Str. 1A, 121, Daugavpils, Latvia*
Corresponding author: Aleksandrs Petjukevičs (aleksandrs.petjukevics@du.lv)

Abstract

This study describes an express method for identifying microorganisms: *Pseudomonas aeruginosa* by standard Raman spectroscopy, without surface-enhanced Raman spectroscopy (SERS). The short-wavelength 514 nm Ar-Ion laser was used for *P. aeruginosa* spectral identification in the Raman shift range from 3200 cm^{-1} to 200 cm^{-1}. The research results showed a high analytical and diagnostic sensitivity of the technology to the express identification of *P. aeruginosa* and can be used as one of the reliable methods. The proven technology is promising for further research of other microorganisms due to several significant advantages of the method. It does not require long-term cultivation of bacteria and special sample preparation, additional expensive reagents or consumables.

Key words: Bacteria, identification of microorganisms, *Pseudomonas aeruginosa*, Raman spectroscopy, reptiles, turtle

Academic editor: Pavel Stoev
Received: 1 September 2023
Accepted: 6 November 2023
Published: 17 November 2023

Citation: Petjukevičs A, Umbraško I, Škute N (2023) Prospects and possibilities of using Raman spectroscopy for the identification of *Pseudomonas aeruginosa* from turtle *Emys orbicularis* (Linnaeus, 1758) skin. BioRisk 21: 19–28. https://doi.org/10.3897/biorisk.21.111983

Introduction

Nowadays, microbiological research is an important and relevant activity in biology and medicine since these studies confirm or deny the presence of certain bacteria with high accuracy and reliability. The classical bacteriological research method and Automated bacteriological diagnostics by different identification systems, VITEK2, Phoenix, MALDI-TOF (matrix-assisted laser description/ionisation time-of-flight mass spectroscopy), Next-generation sequencing, solves the problem of isolating a pure culture of the pathogen with its subsequent identification, but it requires much time and financial investments. Thanks to microbiological research methods, it is possible to establish the causative agents of certain infectious diseases and choose a rational treatment for these diseases (Ramalho et al. 2002). Therefore, developing faster and cheaper routine methods for diagnosing pathogenic microorganisms is a priority area in modern microbiology. *Pseudomonas* spp. is a group of bacteria that can cause several infections. *P. aeruginosa* is the most common disease-causing form of these bacteria, according to the Centers for Disease Control and Prevention (CDC). *P. aeruginosa* belongs to the group of gram-negative bacteria and it is an opportunistic pathogen. Colonies of *P. aeruginosa* consist of rod-shaped bacterium sizes about 1–5 μm long and

0.5–1.0 μm wide (Pauw et al. 2008). They can infect different organs and tissues; the infection is usually severe. Serious infections from *P. aeruginosa* primarily occur in healthcare settings, but people can also become infected from hot tubs and swimming pools or after contact with free-living animals. *P. aeruginosa* is one of the main etiological factors in more than 65% of cases of purulent-septic skin lesions and the fight against these diseases remains an urgent task of modern medicine (Kałużna et al. 2014; Lee et al. 2021; Umbrasko et al. 2022, 2023).

The study of microorganisms that are the causative agents of many infectious diseases is an urgent and important task and progress in solving this can only be achieved if various research methods are used, combining them to obtain the fastest, most reliable and economically justified results (Terrones-Fernandez et al. 2023). The method for detecting microorganisms should not require complex stages of sample preparation while providing rapid identification of the bacteria and be relatively inexpensive and automated. An important criterion for setting up a microbiological study, based on determining the type of bacteria, is its speed. However, the classical bacteriological diagnostic method, based on the isolation and identification of a pure culture of bacteria based on the totality of their specific properties, with all its reliability and information content, is very laborious, financially costly and, most importantly, it is lengthy (it may take several days). In addition to the microbiological method, other laboratory studies allow for obtaining objective information about the microbial composition of the material under study. The use of automated systems with multi-wavelength lasers for the identification of bacteria can speed up the process of microorganism identification by 24–48 hours and obtain reliable information about microorganisms faster (Huang et al. 2004, 2010; Zhu et al. 2014; Pezzotti 2021).

One of the possible methods for the identification of microorganisms is Raman spectroscopy. This method is based on the detection of the molecular structure

Figure 1. Sampling site: Silene Nature Park NATURA2000 (Latvia: 55.690835°N, 26.788760°E).

vibrations of the object and has established itself as a reliable analytical tool in various fields of science (Petjukevičs and Škute 2017; Vaitiekūnaitė and Snitka 2021; Vaitiekūnaitė et al. 2022). It is assumed that bacteria are also characterised by individual spectral lines of Raman scattering (like biomolecule fingerprinting), which make it possible to identify them in a short time (1–2 min) with a very high degree of reliability of the information obtained. In turn, a library of microorganisms is created, based on the spectral information of Raman spectra. Raman spectroscopy makes it possible to apply this method to rapidly identify microorganisms in more comprehensive applications (Patel et al. 2008; Stegelmeier et al. 2019; Kumar et al. 2020; Vaitiekūnaitė et al. 2022). One of the existing problems is the timely delivery of bio-material, as about 30% of bacterial strains do not reach laboratory testing and, thus, cannot be identified. Modern achievements in microbiology using the Raman spectroscopy method and its limitations were considered, as well as the most important world trends in the use of this diagnostic technology for the study and indication of the causative agents of bacterial pathogenic flora and viral infections (Lee et al. 2020; Nakar et al. 2022; Umbrasko et al. 2022).

Based on the preceding, the purpose of this study is to develop an express method for detecting and identifying the bacterium, *P. aeruginosa*, without the use of expensive SERS substrates with metallic gold or silver nanoparticles, based on Raman spectroscopy by analysing and comparing the obtained spectra of analysed samples with the test-control strain: *P. aeruginosa* ATCC 27853 (American Type Culture Collection), as well as optimising the conditions for obtaining spectra and also developing an algorithm for processing primary spectral information.

Materials and methods

Study site, sampling, microbiological identification

For the classic bacteriological method, ten free-living turtles, *Emys orbicularis* (L.) (European pond turtle), were collected and biological material was taken from the skin surface. The sampling site was Silene Nature Park NATURA2000 (Latvia) (55.690835°N, 26.788760°E) (Fig. 1). CliniswabTS Sterile Transport Swabs (Italy) were used to collect samples in wild nature and preserve the microbiological flora for further analysis in the laboratory. Subsequently, *Pseudomonas* spp. was isolated and identified by the classical bacteriological method. Solid nutrient media were used for cultivation and primary microbiological analysis: CHROMagar Orientation and Trypticasein Soy Lab-Agar (BioMaxima S.A., Poland) (Merlino et al. 1996; Garcia and Isenberg 2010). As an objective, daily cultures of the control strain (culture number: *P. aeruginosa* ATCC 27853) and *P. aeruginosa* were taken, which were identified from the skin surface of turtles. Identified colonies from the surface of the skin of turtles were stored in a refrigerator at a temperature of 4 ± 1 °C. Then for the study, the material was warmed up to room temperature 20 ± 1 °C. Bacterial colonies were transferred into 3 ml BHI (Brain Heart Infusion Broth, BioMaxima S.A., Poland) with a disposable sterile loop (COPAN). In the next step, colonies were incubated in a thermostat at 37 ± 1 °C for 24 hours. BHI is a nutrient-rich liquid medium suitable for the inoculation of *P. aeruginosa*. After 24 hours of incubation, the samples were transferred with a sterile disposable viscose swab with a plastic stick (APTACA) to a nutrient medium (Trypticasein Soy Lab-Agar) and incubated in a thermostat at

37 ± 1 °C for 24–48 hours. Isolated colonies were placed in sterile distilled water, the obtained emulsion vortexed ≈ 10 s by Vortex V-1 plus Biosan (Latvia) and visually compared with McFarland 0.5 Standard, 1.5 x 10^8 cells per volume unit (approximate bacterial suspension/ml) and after that, 100 µl of bacterial suspension transferred on sterile microscope 1 – 1.2 mm thick slide (ChannelMED).

Raman spectroscopy of *P. aeruginosa*

Raman scattering spectra were recorded using Renishaw inVia Raman Microscope (United Kingdom), equipped with an optical microscope, Leica DM 2500 (Germany). Raman scattered light from the sample collected through a microscope with a short-distance objective, Leica L 50×/0.50 (eyepiece: HC PLAN 10×/20) and analysed by an inVia Spectrometer. Scattered light focused on a Renishaw air–cooled *Ren Cam* CCD array detector with insertion/retraction speed > 20 mm s^{-1}, repeatability < 0.5 µm, laser spot size ≤ 2 µm FWHM, spatial resolution 2 µm and a field of view > 25µm. During Raman spectroscopy, **>** 50 scans were accumulated for each sample. To improve the noise/signal quality ratio, the laser power was minimised (reduced sample self-fluorescence) and an excitation source Renishaw Stellar-Ren Ar-Ion laser with 514.0 nm wavelength (VIS: 2400 l/mm grating and back-illuminated CCD camera) was used. Lens-focused laser radiation on a quartz glass slide with the sample and Raman spectra were collected by the Raman inVia Reflex microspectroscopy system in the range from 3200 cm^{-1} to 200 cm^{-1} for the full-length spectrum (Fig. 4b) and from 2000 cm^{-1} to 600 cm^{-1} for the short-length spectrum (Fig. 4a). The Ar-Ion laser power was ≤ 50 mW at the laser head and ≤ 0.016 mW at the sample surface (Nova II PD300-3W-V1, Ophir Photonics, Israel). All spectra were read out three times for each bacterial suspension of ten and the results of Raman scattering signals were averaged. All collected data are unsmoothed averages of exposures obtained with an integration time of 2–40 s/exposure. The optimal spectral resolution from the sample surface was reached at 2 cm^{-1}. Data collection was accomplished with Renishaw WiRE 5.5 Raman software, scans, processing (including decomposition of the complex band–shapes analyses) and spectral analysis was controlled by a personal computer. Raman spectral shifts were compared with the Raman spectrum of the control strain (*P. aeruginosa* ATCC 27853) and the S.T. Japan spectral databases, Thermo scientific software, Grams Spectral ID library, Version 9.0.7 and the data from scientific articles.

Results

The results of the research are presented in the form of graphs of the spectral characteristics of *P. aeruginosa* (Fig. 2a) and (Fig. 2b). Ten spectra of *P. aeruginosa* bacterial substances (bacterial colonies suspension, concentration measured according to McFarland 0.5 Standard), systematised and analysed by Raman spectroscopy. In the Raman spectra of control samples, low-intensity lines were detected that were not related to compounds characteristic of bacteria and were taken into account as side noise since the range of detection of Raman shifts and the ratio of line intensities did not correspond to lipids, proteins or nucleic acids. However, it was known that lipids, which are inherent in bacterial cells increasing the reflectivity, also play an important role, probably influencing the intensity level

increase in spectra. It was noted that spontaneous luminescence was absent or was minimal during short-term (up to 60 s) focusing on the sample, which indicates the absence of a noticeable effect of laser radiation on them. Cosmic rays' peaks or unusually high and unstable Raman shifts on the abscissa axis – x was also not considered and was suppressed with cosmic ray removing functions.

The specific Raman spectra observed in this research represent an ensemble of Raman signals that arise from the different molecular vibrations of individual cell components, integrating over nucleic acids, lipids, carbohydrates and proteins. The resulting Raman spectra had a significant number of peaks, for which it was difficult to unambiguously assign to the type of vibrations of groups of atoms in analyte molecules. As can be seen from the graph, the scattered light intensity peaks of this bacterium species coincide in intensity and localisation in the spectral region of Raman scattering in the short and extended spectra for *P. aeruginosa*. The individual Raman shifts were localised at 624 cm^{-1}, 760 cm^{-1}, 808 cm^{-1}, 1002 cm^{-1}, 1032 cm^{-1}, 1145 cm^{-1}, 1150 cm^{-1}, 1178 cm^{-1}, 1207 cm^{-1}, 1330 cm^{-1}, 1359 cm^{-1}, 1445 cm^{-1}, 1580 cm^{-1}, 1600 cm^{-1} and 1620 cm^{-1}; the values and characteristics of the principal obtained components are detailed in table (Table 1).

All obtained spectra from *P. aeruginosa* bacteria had similar characteristics of the values in the studied region 1700–600 cm^{-1} and slightly differ only in the intensity of the peaks. Recorded spectra previously filtered from high-frequency noise (software suppression of cosmic rays) are presented in the paper for further analysis and interpretation. The specific Raman spectra observed here represent an ensemble of signals that arise from the molecular vibrations of individual cell components of gram-negative bacteria, integrating over proteins, lipids and carbohydrates (Fig. 3).

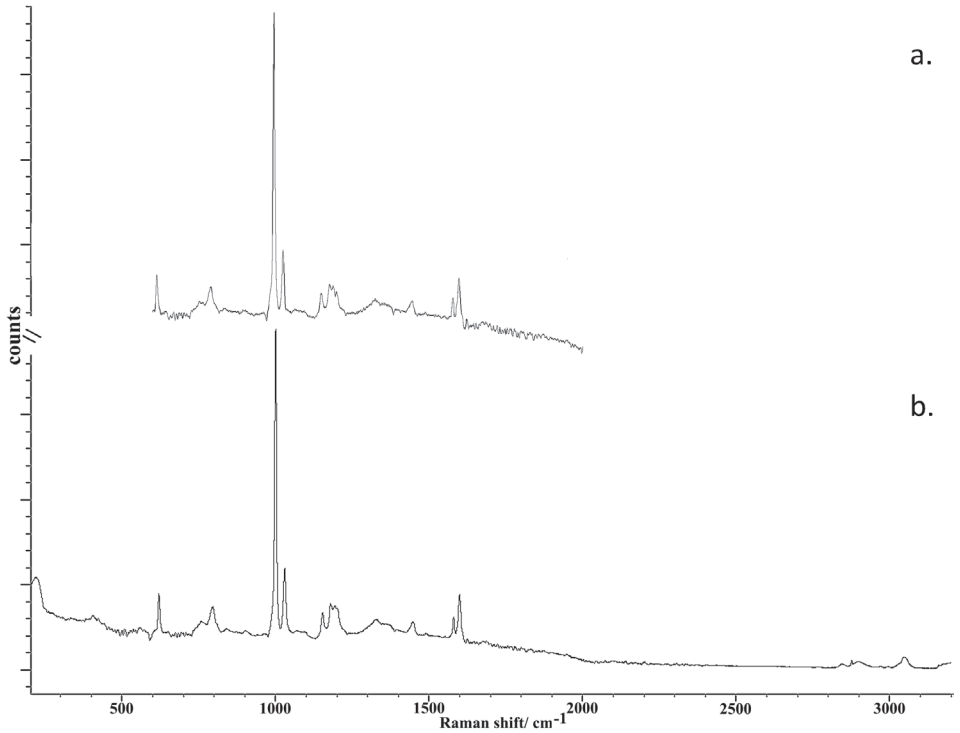

Figure 2. Averaged short-length spectrum: 2000 cm^{-1} – 600 cm^{-1} and extended full-length Raman spectrum: 3200 cm^{-1} – 200 cm^{-1} of *P. aeruginosa* bacteria isolated from turtle skin (**a**) and control strain: *P. aeruginosa* culture number: ATCC 27853 (**b**). On the abscissa axis x– Raman shift (cm^{-1}) along the y-axis is the scattered light intensity (a.u).

Table 1. Raman shifts and tentative assignments of bacteria cells of *P. aeruginosa* isolated from turtle skin.

Raman shifts, (cm^{-1})	Tentative assignment [a]
624	Skeletal vibrations of aromatics rings of amino acid
760	Carbohydrates COO–def, CH_2 rocking
808	Nonpolar amino acids: proline, valine; Polar, uncharged amino acid: υ (CN) tyrosine
1002	amino acid: Phe
1032	C–H in plane, Phe
1145	sulfonic acid residues
1150	Could be associated with the stretching vibration from symmetric glycosidic linkages (C–O–C) and rbr of polysaccharides or C–C str vibrations. ATP
1178	Aromatic amino acids: δ (C–H), Tyr, Phe; Proteins: C–H str Region
1207	Proteins: Amide III, C–C_6H_5 str. Phe, Trp
1330	CH deformations can be assigned to polysaccharides and lipids, as well as to protein
1359	υ(COO–), δ(C–H) proteins
1445	CH deformations can be assigned to polysaccharides and lipids, as well as to protein
1580 (1600–1585)	C=C str, C–C str (in-ring)
1600 (1645–1540)	C–C str (in-ring), Amide II, υ(CN), γ(NH), unsaturated lipids
1620 (1680–1640)	Amide I
650–600	Proteins
1280–1160	B-sheet (proteins)
1333–1313	CH def stretch band
1440–1360	υ(COO–) sym
1460–1440	δ(CH_2) fatty acid molecules without double bonds
1645–1545	Amide II, υ(CN), γ(NH)
2000–1665	Overtones of fundamental or compound vibrations, weak vibrations
3100–2800	C–H str region

[a] Abbreviations: Phe – phenylalanine; Tyr – tyrosine; Trp – tryptophan; rbr – ring breathing; def – deformation; str – stretching; sym – symmetric.

Discussion

The possibility of taking spectra of *P. aeruginosa* directly from the surface of Petri dishes with nutrient agar was initially studied. However, this technology added extra noise to the spectrum due to the agar on which the colonies were grown. The plastic base of the Petri dishes (transparent polystyrene) with nutrient agar on which bacterial colonies were grown (Fig. 4). Raman spectra of *P. aeruginosa* wild type were acquired between 3200 cm^{-1} and 200 cm^{-1}. However, the studies reported here concentrate on vibrational bands found in the fingerprint region 1700 – 600 cm^{-1}. Outside this range, C–H stretching vibrations in the 3050 – 2750 cm^{-1} range dominate spectra. This information is unimportant in this paper, although these Raman bands carry important information about cell membrane fluidity (Huang et al. 2010; Kumar et al. 2020; Pezzotti 2021).

Previously, before Raman scattering, the quality of preparations of the nutrient medium to luminescence capability was checked out. Accordingly, the possibility of the substrate distorting the obtained Raman spectra was neutralised using bacterial suspension drops against direct spectra from the Petri dish surface. The spectra of bacterial suspensions were measured one by one.

Measurements of the bacterial suspension of samples from different groups did not reveal significant differences; however, there was a slight change in the peak height (the intensity of the Raman signal varied depending on the concentration of bacterial suspension in the test sample).

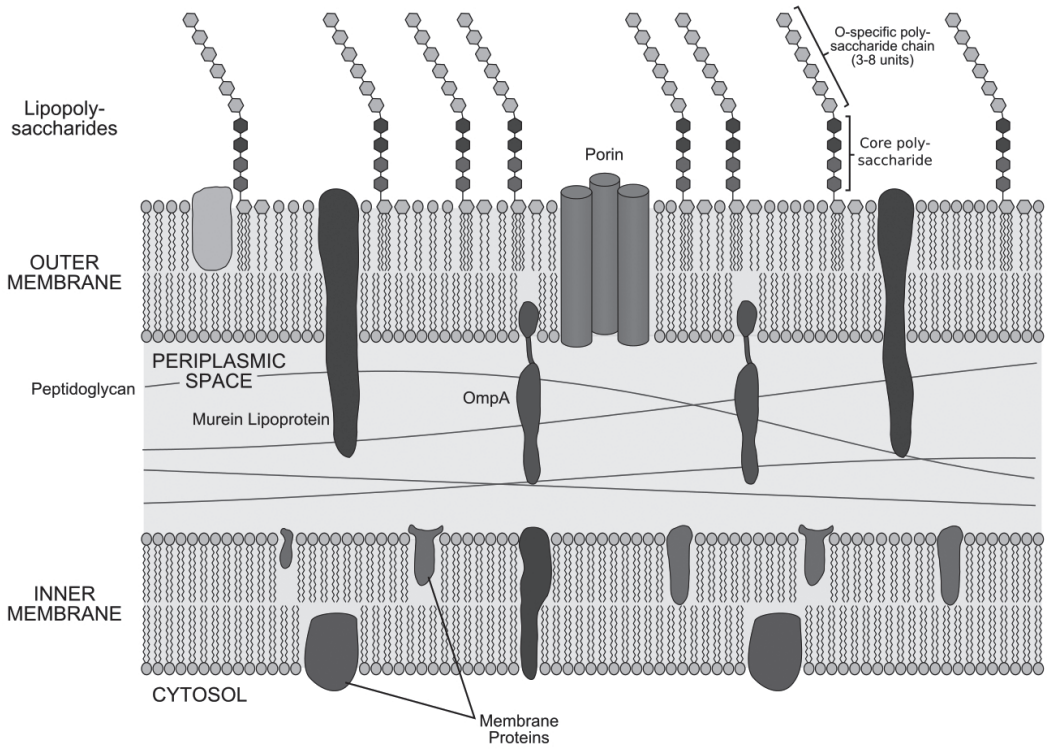

Figure 3. Cell wall components of Gram-negative bacteria (Kagle 2023).

Figure 4. Microscopic image of *Pseudomonas aeruginosa* bacterial cells distribution in agar: (Trypticasein Soy Lab-Agar, BioMaxima).

It was also experimentally confirmed that this bacterial test-suspension by McFarland 0.5 Standard method, 1.5 x 10^8 cells per volume unit, is suitable for Raman spectroscopy during this type of bacterium *P. aeruginosa* analysis and is suitable for Raman spectroscopy without the use of surface signal enhancement technique (SERS).

Each sample of studied bacteria for *P. aeruginosa* is characterised by individual spectral shifts of Raman scattering, which make it possible to identify them in a short time (total time for whole full-range spectrum 1–10 min) and, theoretically, makes it possible to identify a large number of cultures simultaneously. This method is characterised by high sensitivity (100 µl of the prepared suspension according to the McFarland Standard method, 1.5 x 10^8 cells per volume unit) and rapid microorganism identification. The spectra recorded for the same sample remain almost unchanged in the spectrum over a short time, while they could only slightly differ in signal intensity and resolution of the leading bands. It was noted that, to take high-quality, optimally-reproducible spectra, the spectrum from an object should not exceed 60 seconds from one point

Conclusions

The study showed the possibility of obtaining fast and high-quality Raman spectra of *P. aeruginosa* bacterial cells. The used parameters of laser excitation did not cause pronounced destructive changes in bacterial cells. Bacterial cells retained their integrity and cellular organelles with decreased laser beam power. However, the self-luminescence of the samples was reduced to a minimum background effect, which did not significantly affect the quality of the obtained Raman spectra. Laser diagnostics, based on Raman spectroscopy, can be considered an express method for identifying microorganisms and allows detection of the presence of a microorganism even at this concentration (1.5 x 10^8 cells per volume unit). The application of Raman spectroscopy is characterised by high analytical and diagnostic sensitivity and specificity, which is necessary for accurately identifying microorganisms. We can also note the high speed of obtaining results (quantitative and qualitative). The method does not require additional stages of bacterial cultivation or special sample preparation, which are important characteristics for a reliable study and provide analytical reliability and high speed for obtaining results. These advantages of the method give reason to consider it a promising universal express method for microbiological diagnosis of diseases of microbial etiology. The study's results indicate the information content of using Raman spectroscopy to identify microorganisms. However, interpreting these changes and possibly using this technology to study other bacteria requires additional research.

Acknowledgements

We thank the two anonymous reviewers for helpful criticisms that improved the final manuscript.

Additional information

Conflict of interest

The authors have declared that no competing interests exist.

Ethical statement

No ethical statement was reported.

Funding

No funding was reported.

Author contributions

Formal analysis: AP. Investigation: IU. Methodology: IU, AP. Project administration: NŠ. Software: AP. Visualization: AP. Writing – original draft: IU, AP. Writing – review and editing: NŠ.

Author ORCIDs

Aleksandrs Petjukevičs https://orcid.org/0000-0001-6917-2677
Inta Umbraško https://orcid.org/0009-0009-5792-9033
Natalja Škute https://orcid.org/0000-0002-3584-0347

Data availability

All of the data that support the findings of this study are available in the main text.

References

Garcia LS, Isenberg HD (2010) Clinical Microbiology Procedures Handbook (3rd edn. and 2007 updateed). ASM Press, Washington DC. https://doi.org/10.1128/9781555817435

Huang WE, Griffiths RI, Thompson IP, Bailey MJ, Whiteley AS (2004) Raman Microscopic analysis of single microbial cells. Analytical Chemistry 76(15): 4452–4458. https://doi.org/10.1021/ac049753k

Huang WE, Li M, Jarvis RM, Goodacre R, Banwart SA (2010) Shining light on the microbial world: The application of Raman microspectroscopy. Advances in Applied Microbiology 70: 153–186. https://doi.org/10.1016/S0065-2164(10)70005-8

Kagle J (2023) BSC 3271: Microbiology for the Health Sciences. Mansfield University of Pennsylvania, LibreTexts, 672 pp.

Kałużna M, Mikiciński A, Sobiczewski P, Zawadzka M, Zenkteler E, Orlikowska T (2014) Detection, isolation, and preliminary characterization of bacteria contaminating plant tissue cultures. Acta Agrobotanica 66(4): 81–92. https://doi.org/10.5586/aa.2013.054

Kumar S, Gopinathan R, Chandra GK, Umapathy S, Saini DK (2020) Rapid detection of bacterial infection and viability assessment with high specificity and sensitivity using Raman microspectroscopy. Analytical and Bioanalytical Chemistry 412(11): 2505–2516. https://doi.org/10.1007/s00216-020-02474-2

Lee KS, Wagner M, Stocker R (2020) Raman-based sorting of microbial cells to link functions to their genes. Microbial Cell 7(3): 62–65. https://doi.org/10.15698/mic2020.03.709

Lee KS, Landry Z, Pereira FC, Wagner M, Berry D, Huang WE, Taylor GT, Kneipp J, Popp J, Zhang M, Cheng J-X, Stocker R (2021) Raman microspectroscopy for microbiology. Nature Reviews. Methods Primers 1(1): 1–80. https://doi.org/10.1038/s43586-021-00075-6

Merlino J, Siarakas S, Robertson GJ, Funnell GR, Gottlieb T, Bradbury R (1996) Evaluation of CHROMagar Orientation for differentiation and presumptive identification of gram-negative bacilli and *Enterococcus* species. Journal of Clinical Microbiology 34(7): 1788–1793. https://doi.org/10.1128/jcm.34.7.1788-1793.1996

Nakar A, Pistiki A, Ryabchykov O, Bocklitz T, Rösch P, Popp J (2022) Detection of multi-resistant clinical strains of *E. coli* with Raman spectroscopy. Analytical and Bioanalytical Chemistry 414(4): 1481–1492. https://doi.org/10.1007/s00216-021-03800-y

Patel IS, Premasiri WR, Moir DT, Ziegler LD (2008) Barcoding bacterial cells: A SERS based methodology for pathogen identification. Journal of Raman Spectroscopy: JRS 39(11): 1660–1672. https://doi.org/10.1002/jrs.2064

Pauw BD, Walsh TJ, Donnelly JP, Stevens DA, Edwards JE, Calandra T, Pappas PG, Maertens J, Lortholary O, Kauffman CA, Denning DW, Patterson TF, Maschmeyer G, Bille J, Dismukes WE, Herbrecht R, Hope WW, Kibbler CC, Kullberg BJ, Bennett JE (2008) Revised definitions of invasive fungal disease from the European organization for research and treatment of cancer/invasive fungal infections cooperative group and the national institute of allergy and infectious diseases mycoses study group (EORTC/MSG) consensus group. Clinical Infectious Diseases 46(12): 1813–1821. https://doi.org/10.1086/588660

Petjukevičs A, Škute N (2017) Application of Raman scattering in the analysis of the Elodea canadensis genomic dsDNA at different stages of the plant development. Biologia 72(9): 1017–1022. https://doi.org/10.1515/biolog-2017-0120

Pezzotti G (2021) Raman spectroscopy in cell biology and microbiology. Journal of Raman Spectroscopy: JRS 52(12): 2348–2443. https://doi.org/10.1002/jrs.6204

Ramalho R, Cunha J, Teixeira P, Gibbs P (2002) Modified *Pseudomonas* agar: New differential medium for the detection/enumeration of *Pseudomonas aeruginosa* in mineral water. Journal of Microbiological Methods 49(1): 69–74. https://doi.org/10.1016/S0167-7012(01)00365-7

Stegelmeier A, Hoffmann A, Neufeld J (2019) The skin microbiome of vertebrates. Microbiome 7(1): 1–79. https://doi.org/10.1186/s40168-019-0694-6

Terrones-Fernandez I, Casino P, López A, Peiró S, Ríos S, Nardi-Ricart A, García-Montoya E, Asensio D, Marqués AM, Castilla R, Gamez-Montero PJ, Piqué N (2023) Improvement of the pour plate method by separate sterilization of agar and other medium components and reduction of the agar concentration. Microbiology Spectrum 11(1): e0316122. https://doi.org/10.1128/spectrum.03161-22

Umbrasko I, Batjuka A, Petjukevics A, Pupins M, Skute N (2022) Evaluation of microbiome of free-living and Zoo turtles by immunological methods and Raman spectroscopy. 46th FEBS Congress Lisbon (Portugal), July 2022. FEBS Open Bio 12: P-02.4-020. https://doi.org/10.1002/2211-5463.13440

Umbraško I, Batjuka A, Petjukevics A, Pupins M, Skute N (2023) Estimation of *Salmonella* spp. prevalence and diversity among free-living turtles and a zoo collection. Proceedings of the 14th International Scientific and Practical Conference, Rezekne (Latvia), June 2023. Rezekne Academy of Technologies 1: 235–239. https://doi.org/10.17770/etr2023vol1.7267

Vaitiekūnaitė D, Snitka V (2021) Differentiation of Closely Related Oak-Associated Gram-Negative Bacteria by Label-Free Surface Enhanced Raman Spectroscopy (SERS). Microorganisms 9(9): e1969. https://doi.org/10.3390/microorganisms9091969

Vaitiekūnaitė D, Bružaitė I, Snitka V (2022) Endophytes from blueberry (*Vaccinium* sp.) fruit: Characterization of yeast and bacteria via label-free surface-enhanced Raman spectroscopy (SERS). Spectrochimica Acta. Part A: Molecular and Biomolecular Spectroscopy 275: e121158. https://doi.org/10.1016/j.saa.2022.121158

Zhu X, Xu T, Lin Q, Duan Y (2014) Technical development of Raman spectroscopy: From instrumental to advanced combined technologies. Applied Spectroscopy Reviews 49(1): 64–82. https://doi.org/10.1080/05704928.2013.798801

BioRisk

BioRisk 21: 29–40 (2023)
DOI: 10.3897/biorisk.21.111253

Research Article

Study of the dynamics of the microbial communities in the wedge clam *Donax trunculus* (Linnaeus, 1758) from the Bulgarian aquatory of the Black Sea

Sevginar F. Ibryamova[1], Stephany Toschkova[1], Darina Ch. Bachvarova[1], Elitca Stanachkova[1], Radoslav I. Ivanov[1], Nikolay D. Natchev[1,2], Tsveteslava V. Ignatova-Ivanova[1]

1 *Department of Biology, Shumen University "Konstantin Preslavski", Department of Biology 115 Universitetska Str., Shumen, Bulgaria*

2 *Unit for Integrative Zoology, Department of Evolutionary Biology, University of Vienna, Djerassiplatz 1, 1030 Vienna, Austria*

Corresponding author: Tsveteslava V. Ignatova-Ivanova (ts.ignatovaivanova@shu.bg)

Abstract

In the present work, we investigated the dynamics of the microbial communities in the wedge clam *Donax trunculus* (Linnaeus, 1758) from the Bulgarian coastal waters of the Black Sea. The samples were collected in the period of January 2020 until December 2022 from Arkutino, Ahtopol, Obzor and Tsarevo. The BIOLOG system was used for microbiological determination. In our investigation were isolated the following microorganisms: *Enterococcus cancerogenus*, *Enterococcus hirae*, *Escherichia vulneris*, *Citrobacter farmeri*, *Acinetobacter gyllenbergii*, *Enterococcus hirae*, *Escherichia vulneris*, *Enterobacter cloacae*, *Escherichia hermannii*, *Pseudomonas mendocina*, *Pseudomonas fulva*, *Pseudomonas alcaligenes*, *Pseudomonas putida*, *Acinetobacter johnsonii*, *Acinetobacter gyllenbergii*, *Enterococcus hirae*, *Escherichia vulneris*, *Enterococcus gallinarum*, *Citrobacter sedakii*, *Pseudomonas putida*, *Streptococcus lugdunensis*, *Enterococcus casseliflavus*, *Vibrio cincinnatiensis*, *Vibrio alginolyticus*, *Vibrio parahaemolyticus*, *Enterococcus hirae*, *Streptococcus aureus*, *Staphylococcus lugdunensis* and *Enterococcus casseliflavus*. During the winter period, we detected the presence of *Pseudomonas sp.* – *P. alcaligenes*, *P. putida*, and *A. gyllenbergii.* In the autumn months we isolated *C. sedakii*, *C. farmeri*, *A. gyllenbergii*, *A. johnsonii*, *P. fulva* and *E. casseliflavus.* In the spring, *E. cancerogenus*, *E. hirae* and *Pseudomonas mendocina* were found. During the summer, the highest biodiversity of microorganisms - *E. hirae*, *E. vulneris*, *E. cloacae*, *E. gallinarum*, *P. putida*, *V. cincinnatiensis*, *V. alginolyticus*, *V. parahaemolyticus*, *S. aureus*, *E. hermannii* and *S. lugdunensis* were registered. Although our three-year research showed that some species are permanent and others are transient, we tend to accept the conclusion that there is only a transient microbiota in mussels and it changes depending on environmental conditions or is a result of pollution of the Black Sea.

Key words: Bivalves, hydrobiology, microbial identification, molluscs, pathogens, pollutions

Academic editor: Pavel Stoev
Received: 16 August 2023
Accepted: 13 October 2023
Published: 5 December 2023

Citation: Ibryamova SF, Toschkova S, Bachvarova DC, Stanachkova E, Ivanov RI, Natchev ND, Ignatova-Ivanova TV (2023) Study of the dynamics of the microbial communities in the wedge clam *Donax trunculus* (Linnaeus, 1758) from the Bulgarian aquatory of the Black Sea. BioRisk 21: 29–40. https://doi.org/10.3897/biorisk.21.111253

Introduction

The wedge clam *Donax trunculus* (Linnaeus, 1758) is found in the entire region of the Black Sea coast, but according to Fernández-Pérez et al. (2017) its population is extremely high on the territory of the Bulgarian Black Sea aquatory.

The species occurs in the Mediterranean and the Black Seas, and in the Atlantic Ocean from Senegal to the North Atlantic coast of France (Deval 2009). The species inhabits open sandy beaches where it forms thick beds, as the highest density are at depths from 0 to 3 m. It is considered a warm-water temperate species (Bayed and Guillou 1985; Lamine et al. 2020a; Chahouri et al. 2022).

The shellfish are exposed to diseases caused by various bacteria, which can cause a mass extinction of the species. It was detected that the cause of outbreaks of diseases in bivalves is related to conditional pathogens, i.e. free-living pathogenic bacteria which, under favourable conditions, can cause diseases. This poses a serious risk to humans as consumers of bivalve species. Pathogenic bacteria can enter into the clams directly from seawater, from the microalgae they feed on, but also as a result of anthropogenic pollution of the environment. For *D. trunculus*, various studies indicate it importance for the assessment and monitoring of the ecological conditions of the sandy beaches (Moukrim et al. 2004; Idardare et al. 2008; Nadir et al. 2015; Lamine et al. 2020b). *D. trunculus* can be used as an indicator species to understand population dynamics and to interpret variation in various biological parameters used as biomarkers of pollution. The dynamics of the microbial population of *D. trunculus* in the Black Sea Region have not been studied and there are no data concerning the microbial communities inhabiting the bivalves. Our study contributes to the study of microbiota of the Black Sea. It should be linked to additional long-term studies to provide basic information for the development of strategies for the protection and monitoring of the Black Sea coastal ecosystem. In a previous study, the microbial variation in the Arkutino Region was described (Ibryamova et al. 2022a). Our results demonstrated the presence of bacterial species of genera *Pseudomonas*, *Enterococcus*, *Escherichia*, *Citrobacter* and *Acinetobacer* in wedge clams *Donax trunculus* (Linnaeus, 1758). In the present study, only the species *D. trunculus* was investigated, as it was the only one found in the surveyed area. We found that the concentrations of *E. vulneris* exceed by 190 times the maximum available values according to Ordinance No. 4/20.10.2000. Increased concentrations of coliforms in the summer indicate a seasonal worsening of the conditions of the seawater as a consequence of anthropogenic activity. The main goal of the present work was to investigate the dynamics of microbial communities in the wedge clam *D. trunculus* (Linnaeus, 1758) from the Bulgarian Black Sea aquatory.

Materials and methods

Place and duration of the study

The study was conducted at the Department of Biology, University of Shumen, Bulgaria, from January 2020 until December 2022. The samples were collected from the regions of Mussel farms – Arkutino, Ahtopol, Obzor and Tsarevo (Fig. 1).

Collection of samples

After collection of three subsamples (each of about 1 kg), the mussels were refrigerated (4 °C) and transported to the laboratory for further immediate analysis, without freezing the specimens. In this study, we examined wedge clams of similar size, weight and shape to ensure maximal uniformity in the applied

Figure 1. Sampling locations at the Black Sea coast.

methods (Duquesne et al. 2004). The average length of mussels used in the study was 2.2 ± 0.43 cm. The mussels used for the analysis were collected monthly, throughout the three-year period. The collection of samples was carried out by trawling by JSC "Black Sea Fishing", Burgas.

Microbiological analyses

The mussels were scrubbed free of dirt, washed in hypochlorite solution (20 mg l^{-1}), rinsed with sterile distilled water and shucked with a sterile knife. The whole soft tissues of the mussel's liquor samples (about 100 g) were homogenised.

Faecal coliforms (FC) were enumerated through five tubes per dilution most probable number (MPN) series (Ignatova-Ivanova et al. 2018). After 3 h at 37 °C plus 21 h at 44 °C, gas positive tubes were recorded for FC. From each of the FC gas positive tubes, 0.1 ml were transferred in tubes with 10 ml of Tryptone Water (Oxoid, Basingstoke, UK) and then incubated for 24 h at 44 °C. *E. coli* were enumerated by MacConkey agar (Merck, Darmstadt, Germany). The plates were incubated aerobically at 35–37 °C for 18–24 hours. *E. coli* grows matte dark pink to tile-red colonies, surrounded by an opaque area due to the precipitation of salts in this environment. *Pseudomonas* sp. were enumerated by Cetrimide Agar (Merck KGaA, 64271 Darmstadt, Germany). Lactic acid bacteria (LAB) were isolated in media of MRS (de Mann Rogosa Sharpe, Biolife 272-20128, Milano, Italia). The strains were cultured overnight (16–18 h) on MRS at 37 °C and in limited oxygen (tubes or Petri dishes with the strains were incubated in plastic bags, which limited the oxygen content). When determining the number of isolated species of microorganisms, the number of cells in 1 ml of sample was calculated, after which the percentage of the total number of microorganisms in the sample was calculated for each isolated species.

Microbial identification databases for the "BIOLOG" system

The microbial identification was performed by the BIOLOG Microbial Identification System VIO45101AM. The isolated strains were screened on BL4021502

Tryptic Soy Agar (TCA), cultured for 24 hours at 37 °C and then subjected to Gen III plaque identification to identify Gram positive and Gram negative aerobic bacteria. The microscopic pictures were performed using stereomicroscope OPTIKA (Italy) with a DinoEye, Eyepiece camera with 5 megapixels. The photographs were performed by using a Canon EOS 60D camera. The GEN III MicroPlate test panel provides a standardised micromethod using 94 biochemical tests to profile and identify a broad range of Gram-negative and Gram-positive bacteria. BIOLOG's Microbial Identification Systems software (e.g. OmniLog Data Collection) was used to identify the bacterium from its phenotypic pattern in the GEN III MicroPlate. The BIOLOG system allows to quickly and accurately identify more than 2900 species of aerobic and anaerobic bacteria, yeasts and fungi. BIOLOG's advanced phenotypic technology provides valuable information for the properties of the strains, in addition to species-level identification. BIOLOG's carbon technology identifies the environment and pathogenic microorganisms by producing a characteristic pattern or "metabolic fingerprint" of discrete test reactions performed in a 96-well microplate. The culture suspensions are tested with a panel of pre-selected assays, then incubated, read and compared with extensive data-bases (https://www.biolog.com/products-portfolio-overview/microbial-identification).

Results

The isolated species of microorganisms by year and percentage are presented in Figs 2–5. The species *E. cancerogenus*, *E. hirae*, *E. vulneris*, *C. farmeri* and *A. gyllenbergii* were isolated from the Arkutino Region (Fig. 2). The species *E. cancerogenus* was isolated only in 2020 in the month of May. The species *E. hirae* was isolated in all three years, with the highest percentage recorded in 2021 - 60.71% and the lowest in 2020 - 21.25%. This species was isolated during the months of May, June and August. The species *E. vulneris* was isolated in all three years, with the highest percentage reported in 2022 - 20.15% and, in 2020 and 2021, the percentage was 11.69%. The species was isolated

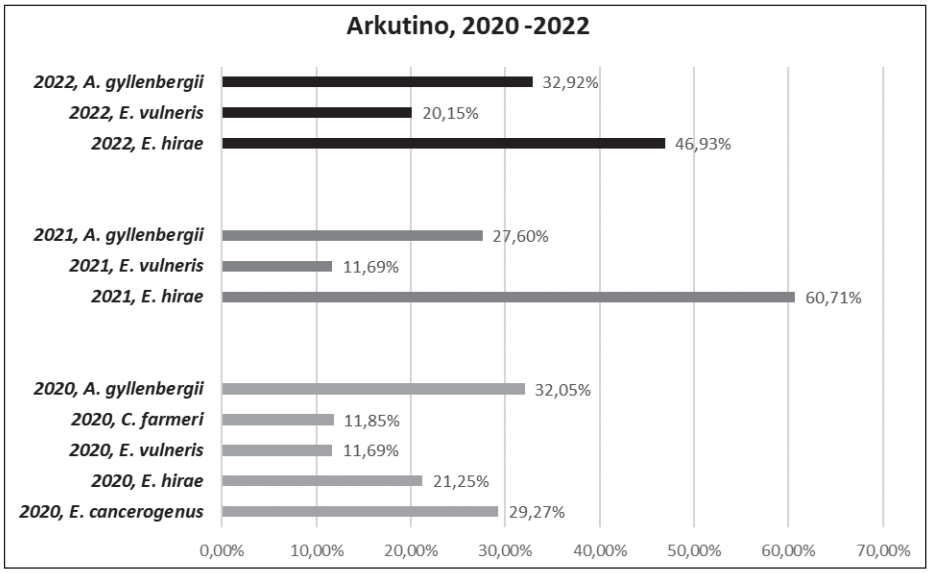

Figure 2. Microbial population dynamics in the Arcutino Region.

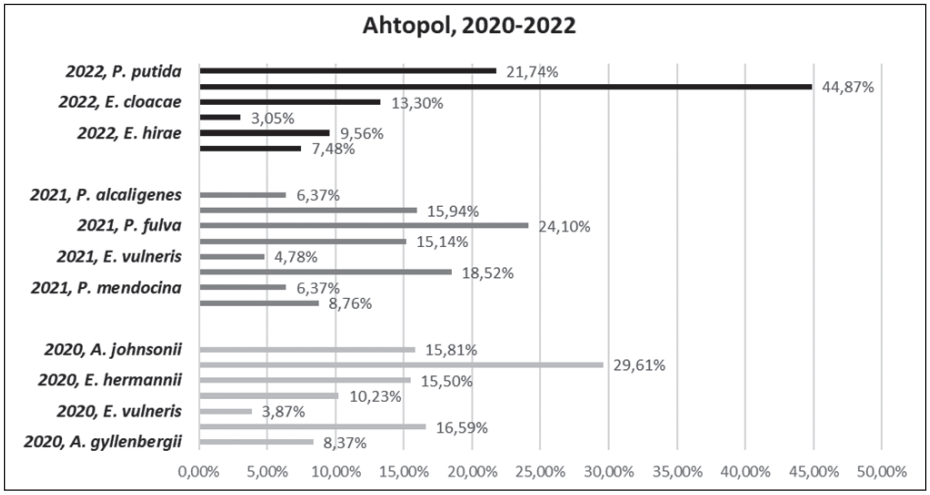

Figure 3. Microbial population dynamics in the region of Ahtopol.

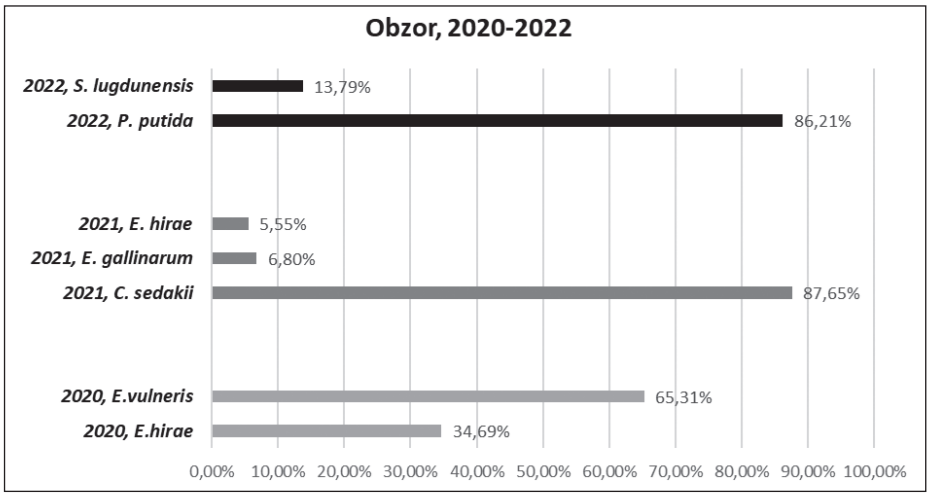

Figure 4. Dynamics of the microbial population in the Obzor Region.

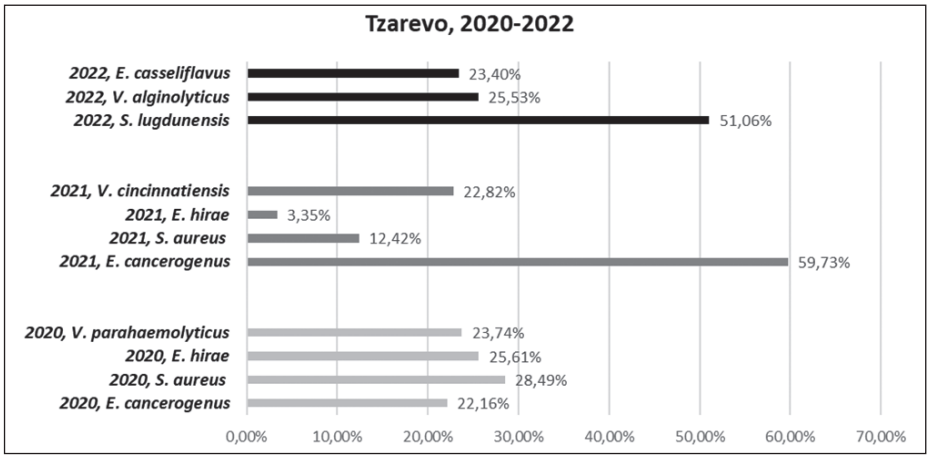

Figure 5. Dynamics of the microbial population in the region of Tsarevo.

in the months of June and August. The species *C. farmeri* was isolated only in 2020 in the month of September. The species *A. gyllenbergii* was isolated in all three years, with the highest percentage reported in 2022, 32.92% and the

lowest in 2021, 27.60%. The species *A. gyllenbergii* was isolated in the month of October.

The species *E. hirae*, *E. vulneris*, *E. cloacae*, *E. hermannii*, *P. mendocina*, *P. fulva*, *P. alcaligenes*, *P. putida*, *A. johnsonii* and *A. gyllenbergii* were isolated from the Ahtopol Region (Fig. 3). The species *E. hirae* was isolated in all three years, in the month of June. The highest percentage was reported in 2021 - 18.52% and the lowest percentage in 2022 - 9.56%. The species *E. vulneris* was isolated in all three years, in the months of June and July. The highest percentage was reported in 2021 - 4.78% and the lowest in 2022 - 3.05%. The species *E. cloacae* was isolated in all three years, in the month of August. The highest percentage was reported in 2021 - 15.14% and the lowest in 2020 - 10.23%. The species *E. hermannii* was isolated in 2020 and 2022, in the months of August and September. The highest percentage was reported in 2022 - 44.87%. The species *P. mendocina* was isolated only in 2021, in the month of May. The species *P. fulva* was isolated only in 2021, in the month of September. The species *P. alcaligenes* was isolated in 2020 and 2021, in the months of November and December. In 2020, its percentage was significantly higher 29.61% compared to 6.37% in 2021. The species *P. putida* was isolated in 2021 and 2022, in the month of December. In 2021, the amount was 15.94% and in 2022 - 21.74%. The species *A. johnsonii* was isolated only in 2020, in the month of October. The species *A. gyllenbergii* was isolated in all three years, in the month of February. The percentage of the species is between 7.5 and 8.7% of the total sample.

The species *E. hirae*, *E. vulneris*, *E. gallinarum*, *C. sedakii*, *P. putida* and *S. lugdunensis* were isolated from the Obzor Region (Fig. 4). The species *E. hirae* was isolated in 2020 - 34.69% and 2021 - 5.55%, in the months of July and November. The species *E. vulneris* was isolated only in 2020 in the month of July at a relatively high percentage of 65.31% of the total sample. The species *E. gallinarum* was isolated only in 2021 in the month of July at a relatively low percentage of 6.80% of the total sample. The species *C. sedakii* was isolated only in 2021 in the month of September at a relatively high percentage of 87.65% of the total sample. The species *P. putida* was isolated only in 2022 in the month of August at a relatively high percentage of 86.21% of the total sample. The species *S. lugdunensis* was isolated only in 2022 in the month of August at a relatively low percentage of 13.79% of the total sample.

The species *E. casseliflavus*, *Vibrio cincinnatiensis*, *V. alginolyticus*, *V. parahaemolyticus*, *E. hirae*, *S. aureus*, *S. lugdunensis* and *E. casseliflavus* were isolated from the Tsarevo Region (Fig. 5). The species *E. casseliflavus* was isolated only in 2022, in the month of September at 23.40% of the total sample. The species *V. cincinnatiensis* was isolated only in 2021, in the month of August at 22.82% of the total sample. The species *V. alginolyticus* was isolated only in 2022, in the month of August at 25.53% of the total sample (Fig. 6a). The species *V. parahaemolyticus* was isolated only in 2020, in the month of August at 25.53% of the total sample (Fig. 6b). The species *E. hirae* was isolated only in 2020, in the month of August at 25.53% of the total sample. The species *S. aureus* was isolated only in 2021, in the month of August at 12.42% of the total sample. The species *S. lugdunensis* was isolated only in 2022, in the month of August at 51.06% of the total sample. The species *E. casseliflavus* was isolated only in 2022, in the month of September at 23.40% of the total sample.

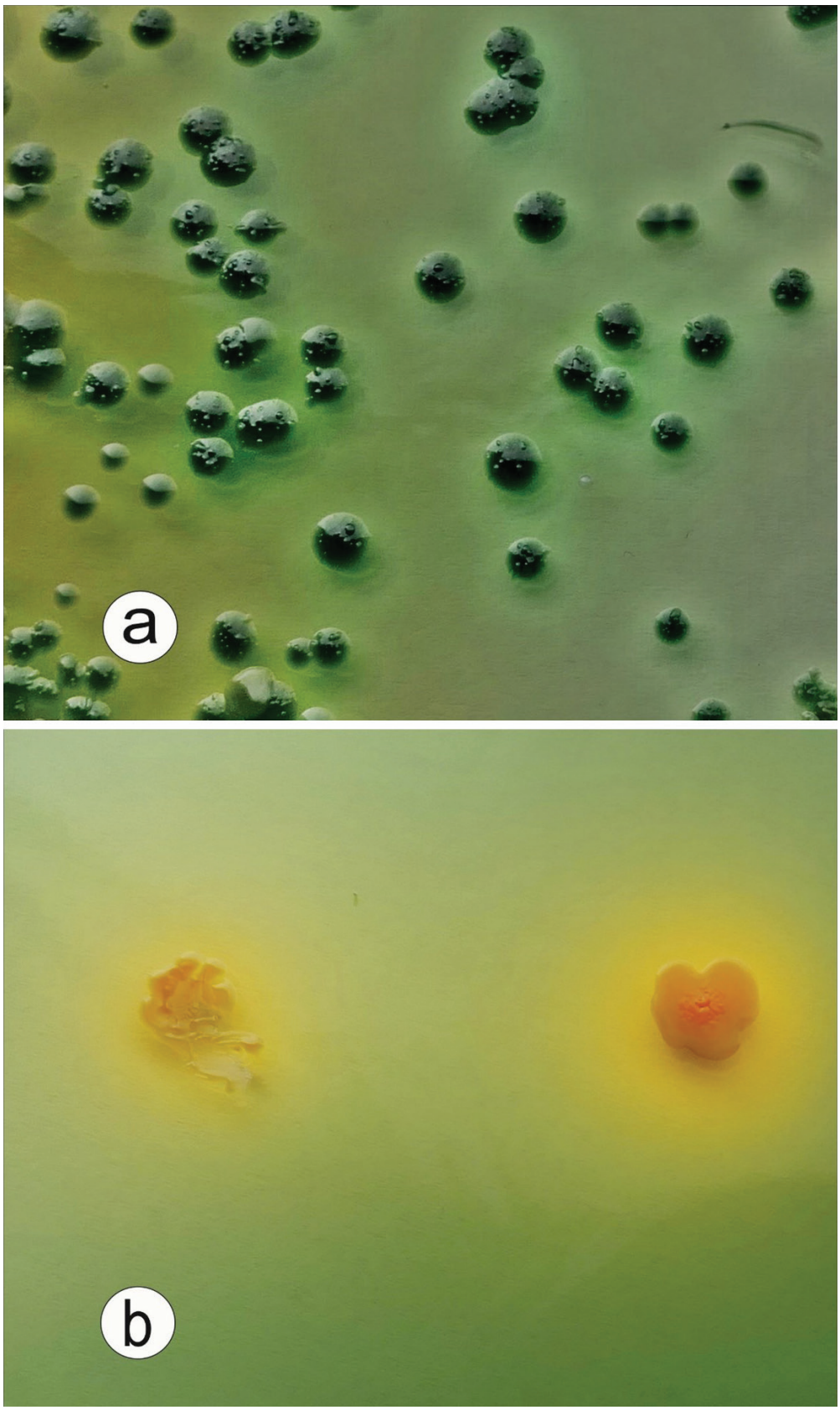

Figure 6. Microscope picture of the colonies of the isolated species *a*) *Vibrio alginolyticus* and b) *Vibrio parahaemolyticus.* The picture was taken using the microscope OPTIKA (Italy) and DinoEye, Eyepiece camera, USB, 1.3 megapixsel, up to 5 megapixels.

Discussion

According to our results, the microbiota found in mussels can be considered in two types. The so-called autochthonous microbiota, which was stable and permanently present, independent of changes in environmental conditions. The allochthonous (transient) microbiota, was entirely dependent on environmental conditions and was related to the change in these conditions. On the basis of our investigation, we can state that the species *E. hirae* (from the end of the spring and during the summer), *E. vulneris* (during the summer) and *A. gyllenbergii* (in the autumn), which were isolated in all three years, represented autochthonous microflora for the Arkutino area. In contrast, the species *E. cancerogenus* (isolated only in May) and *C. farmeri* – detected in September, were considered transitional species. In our previous research (Ibryamova et al. 2022a), we detected a significant increase in the quantity of the coliforms in the region of Arkutino in July 2020, when the quantity of the faecal coliforms was 190 times over the norms prescribed in Ordinance No. 4/20.10.2000 (the number of FC in the inter-shell content should be less than 300 NVB). Two years later, the tendency for a high titter of faecal coliforms was maintained. In 2022, the amount increased by 50%, which, according to the regulation, showed more than 250 times the sanitary accepted amount.

E. vulneris is an opportunistic human pathogen. It was reported primarily in elderly patients and invasive infections have been observed in immunocompromised persons. *E. vulneris* can cause severe diarrhoea and sepsis in infants (Jain et al. 2016). *E. vulneris* has limited clinical reports of human infections worldwide. In humans, *E. vulneris* was originally isolated from infected wounds, along with other bacteria such as *Staphylococcus aureus*, *S. epidermidis*, streptococci, enterococci and *Enterobacter* spp., *Acinetobacter lwoffii* and *Cedecea neteri.* Later, *E. vulneris* was also isolated from other clinical samples, such as faeces, sputum, urine, vaginal and throat swabs, where it was believed to be a coloniser (Jain et al. 2016). Isolation of this species firstly indicates anthropogenic contamination and the consumption of mussels with such a high content of microorganisms of this species can have a serious effect on human health.

The presence of *E. vulneris* was permanent and that species may have become part of the autochthonous microflora as a result of anthropogenic activity and environmental pollution from the hotels and resorts in the area - the species was mainly isolated during the active summer season - from June to August.

The most diverse microorganisms were isolated from the Ahtopol Region. Of these, autochthonous species, detected in all three years were: *E. hirae*, *E. vulneris*, *E. cloacae* and *A. gyllenbergii*. The species *E. hermannii*, *P. mendocina*, *P. fulva*, *P. alcaligenes*, *P. putida* and *A. johnsonii* were considered allochthonous. As in the Arkutino Region, we registered an increase over the allowed amounts of faecal coliforms (under Ordinance No. 4/20.10.2000) during the summer season until the end of September. In the region of Ahtopol, two species of the genus Escherichia sp. were detected – *E. hermannii* and *E. vulneris*. The species of *Pseudomonas* sp. were isolated during the cold months. Presumably, the different species of the genus *Pseudomonas* sp. appeared because of accidents related to changes in the direction of sea currents and variations in the water temperature or pH. However, it can also be speculated that the genus *Pseudomonas* sp. is autochthonous to the mussels *D. trunculus*, as some

species may be allochthonous. Jorquera et al. (2001) suggested that the bivalves contain only "transition" microbiota. We confirm partly such hypothesis for *Acinetobacter* sp. – the genus was autochthonous and some of the species were transient.

In the region of Obzor, where there was no active summer touristic season, only a few species of the microorganisms were isolated. All microorganism species were transient, as there was not a single species that was isolated regularly in all of the three years. Only three species of *Vibrio* sp. were isolated from the region of Tsarevo. We can attribute all three species to the transitional microbiota and connect them to the anthropogenic factors, since they were isolated only in the month of August. All other species were isolated sporadically in all of the three years of our investigation and no time pattern was detected.

In our opinion, allochthonous microbiota can enter mussels as a result of environmental pollution of different origins - natural, due to changes in climate, temperature, salinity, currents or as a result of human activity. Considering that the mussels are the filter of the sea, many microorganisms enter them during feeding. In 1960, Colwell and Liston showed a high percentage of the presence of the species *Pseudomonas* sp., *Vibrio* sp., *Flavobacterium* sp. and *Achromobacter* sp. in the Pacific oyster (*Crassostrea gigas*). Most of the studies since then were concentrated on the pathogens that cause shellfish diseases. The best studied pathogenic species belonged to *Vibrio* sp. For example, *V. tapetis* received special attention since it caused Brown Ring Disease (BRD), the bacterial etiology which is described in adult clams. In addition, the disease caused by it is considered one of the main limiting factors for the colonies of the Manila clams (*Venerupis philippinarum*) and was also detected in cultured clams in Korea (Europe-Borrego et al. 1996; Park et al. 2006). In this regard, the fact of the appearance of *Vibrio* sp. (Fig. 6a, b) in one of the most visited seaside resorts - Tsarevo, is disturbing. This may indicate the spread of mussel disease in this area. In our previous study on the influence of water parameters on the occurrence of transient microbiota in mussels (Ibryamova et al. 2022b), we showed that, as seawater salinity decreases, transient species and faecal coliforms appeared in the probes.

A study by Romalde et al. (2012) demonstrated that the genus *Pseudomonas* sp. is one of the main groups of microbiota in mussels, although some seasonal variations can be observed. Presumably, these variations are related to the environment impacts on the sea water - temperature, pH and water conductivity changes. These authors also stated that wide diversity of *Pseudomonas* species occurred sporadically, which also correlates with our results from the Ahtopol Region.

Previous research on different fish species from the Bulgarian Black Sea aquatory showed that the *Pseudomonas* species are of key importance for the ichthyofauna and are a permanent part of the composition of the fish microbiota (Ibryamova et al. 2022b). In mussels, however, the result was different. Despite the limited amount of data, we suggest that the clam *D. trunculus* does not have a permanent intrinsic microbiota, but only a transient one. The fact that completely different species of microorganisms have been isolated from geographically rather close regions, such as Ahtopol, Arkutino and Tsarevo for a long period of time (3 years) proves that hypothesis. Our results indicate that the anthropogenic factors may impact to a large degree the composition of the microbiota in mussels.

Conclusion

When studying bivalves, it is very important to know their microbiological composition, in order to be able to evaluate the various diseases related to consumption of these organisms by humans. Many species inhabiting the Black Sea feed on wedge clams, which, if infected by a certain type of microorganism, can cause imbalances in the populations. This could prove potentially fatal for the fragile ecology of the Black Sea. Our results regarding the dynamics of the microbial population in *D. trunculus* showed that some species of microbial pathogens were permanent and others were transient. Despite the fact that we detected rather regularly some species of microorganisms, we tend to accept the idea that there is only a transient microbiota in mussels and it changes depending on environmental conditions or may be a result of pollution of the Black Sea. We cannot exclude, however, that *D. trunculus* developed symbiosis with some species of bacteria and use them as a source of vitamins and minerals. Further investigations will verify or disprove this hypothesis.

Additional information

Conflict of interest

The authors have declared that no competing interests exist.

Ethical statement

No ethical statement was reported.

Funding

This study was financially supported by the National Research Fund of the Bulgarian Ministry of Education and Science (Grant- H31/6 KP-06-H31/6/10.12.19) and by Shumen University, Department of Biology (Grant 08-113/20.02.2023).

Author contributions

Sevginar F. Ibryamova, Stephany Toschkova, Darina Ch. Bachvarova, Elitca Stanachkova - microbiological analysis, Radoslav I. Ivanov and Nikolay D. Natchev - delivery of mussels by trawling, Tsveteslava V. Ignatova-Ivanova - writing the article and its concept.

Data availability

All of the data that support the findings of this study are available in the main text. The data underpinning the analysis reported in this paper are deposited at “Data repository” at https://doi.org/10.3897/biorisk.21.111253.

References

Bayed A, Guillou J (1985) A contribution to the study of populations of the *Donax* genus: the population of *D. trunculus* L. (Mollusca, Bivalvia) from Mehdia (Morocco). Annales de l’Institut Océanographique (Monaco) 61(2): 139–147. https://api.semanticscholar.org/CorpusID:131834201

Borrego JJ, Castro D, Luque A, Paillard C, Maes P, García M, Ventosa A (1996) *Vibrio tapetis sp*. nov., the causative agent of the brown ring disease affecting cultured

clams. International Journal of Systematic Bacteriology 46(2): 480–484. https://doi.org/10.1099/00207713-46-2-480

Chahouri M, Agnaou M, El Hanaoui M, Yacoubi B, Moukrim A, Banaoui A (2022) Hanaoui El, Yacoubi B, Moukrim A, Banaoui A Assessment of seasonal and spatial variation responses of integrated biomarkers in two marine sentinel bivalve species: Agadir Bay (Southern of Morocco). Marine Pollution Bulletin 174: 113179. https://doi.org/10.1016/j.marpolbul.2021.113179

Deval MC (2009) Growth and reproduction of the wedge clam (*Donax trunculus*) in the Sea of Marmara, Turkey. Journal of Applied Ichthyology 25(5): 551–558. https://doi.org/10.1111/j.1439-0426.2009.01258.x

Duquesne S, Liess M, Bird DJ (2004) Sub-lethal effects of metal exposure: Physiological and behavioral responses of the estuarine bivalve *Macoma balthica*. Marine Environmental Research 58(2–5): 245–250. https://doi.org/10.1016/j.marenvres.2004.03.066

Fernández-Pérez J, Froufe E, Nantón A, Gaspar MB, Méndez J (2017) Genetic diversity and population genetic analysis of *Donax vittatus* (Mollusca: Bivalvia) and phylogeny of the genus with mitochondrial and nuclear markers. Estuarine, Coastal and Shelf Science 197: 126–135. https://doi.org/10.1016/j.ecss.2017.08.032

Ibryamova S, Pavlova B, Stanachkova E, Salim S, Lyatif A, Dimitrov D, Bachvarova D, Chipev N, Natchev N, Ignatova-Ivanova T (2022a) Seasonal variations of the microflora of wedge clam *Donax trunculus* (Linnaeus, 1758) from the region of Arkutino (Bulgarian Black Sea aquatory). BioRisk 17: 253–262. https://doi.org/10.3897/biorisk.17.77097

Ibryamova S, Toschkova S, Pavlova B, Stanachkova E, Ivanov R, Natchev N, Chipev N, Ignatova-Ivanova T (2022b) A study of the microbiology of the intestinal tract in different species of Teleost fish from the Black Sea. BioRisk 18: 105–113. https://doi.org/10.3897/biorisk.18.80357, https://biorisk.pensoft.net

Idardare Z, Chiffoleau JF, Moukrim A, Ait Alla A, Auger D, Lefrere L, Rozuel E (2008) Metal concentrations in sediment and *Nereis diversicolor* in two Moroccan lagoons: Khniffis and Oualidia. Chemistry and Ecology 24(5): 329–340. https://doi.org/10.1080/02757540802378774

Ignatova-Ivanova T, Ibrjmova S, Stanachkova E, Ivanov R (2018) Microbiological characteristic of microflora of (*Mytilus galloprovincialis* Lam.) in The Bulgarian Black Sea aquatory. Research Journal of Pharmaceutical, Biological and Chemical Sciences 9(1): 199–205. https://www.rjpbcs.com/pdf/2018_9(1)/[29].pdf

Jain S, Nagarjuna D, Gaind R, Chopra S, Debata PK, Dawar R, Sardana R, Yadav M (2016) Escherichia vulneris: An unusual cause of complicated diarrhoea and sepsis in an infant. A case report and review of literature. New Microbes and New Infections 13: 83–86. https://doi.org/10.1016/j.nmni.2016.07.002

Jorquera MA, Silva FR, Riquelme CE (2001) Bacteria in the culture of the scallop *Argopecten purpuratus* (Lamarck, 1819). Aquaculture International 9(4): 285–303. https://doi.org/10.1023/A:1020449324456

Lamine A, Alla A, Ben Haddad M, El Habouz H, Nadir M, Moukrim A (2020a) Population dynamics of donax trunculus on the sandy beach of Taghazout (southern Morocco). Regional Studies in Marine Science 33: 100912. https://doi.org/10.1016/j.rsma.2019.100912

Lamine I, Alla AA, Hadad MB, Habouz HEl, Nadir M, Moukrim A (2020b) Population dynamics of *Donax trunculus* on the sandy beach of Taghazout (southern Morocco). Regional Studies in Marine Science 33: 100912. https://doi.org/10.1016/j.rsma.2019.100912

Moukrim A, El Hamidi F, Lagbouri A, Kaaya A, Zekhnini A, Bouhaimi A, Narbonne JF (2004) Study of *Donax trunculus* as a sentinel species for environmental monitoring of sandy beaches on Moroccan coasts. Bulletin of Environmental Contamination and Toxicology 73(4): 674–681. https://doi.org/10.1007/s00128-004-0479-9

Nadir M, Agnaou M, Idardare Z, Chahid A, Bouzid T, Moukrim A (2015) Impact study of M'zar submarine emissary (Agadir Bay, Morocco): Trace metals accumulation (Cd, Pb and Hg) and biochemical response of marine Mollusk *D. trunculus* (Linnaeus, 1758). Journal of Materials & Environmental Sciences 6(8): 2292–2300. https://www.jmaterenvironsci.com/Document/vol6/vol6_N8/274-JMES-1605-2015-Nadir.pdf

Park KI, Paillard C, Le Chevalier P, Choi KS (2006) Report on the occurrence of brown ring disease (BRD) in Manila clam, *Ruditapes philippinarum*, on the west coast of Korea. Aquaculture (Amsterdam, Netherlands) 200(1–4): 610–613. https://doi.org/10.1016/j.aquaculture.2005.12.011

Romalde JL, Diéguez AL, Doce A, Lasa A, Balboa S, López C, Beaz-Hidalgo R (2012) Advances in the knowledge of the microbiota associated with clams from natural beds, Chapter 7, Clam fisheries and aquaculture. Nova publishers, New York, 163 pp.